

Material transport in the frame of PSI

K. Krieger

with contributions from many colleagues (credits inside)

Association EURATOM Max-Planck Institut für Plasmaphysik, Boltzmannstr. 2, 85748 Garching, Germany

Overview and rationale

Material transport processes

Particle collisions

Plasma turbulence

Experiments

Phenomenological observations

Specific experiments

Summary and outlook

Overview and rationale

Material transport processes

Particle collisions

Plasma turbulence

Experiments

Phenomenological observations

Specific experiments

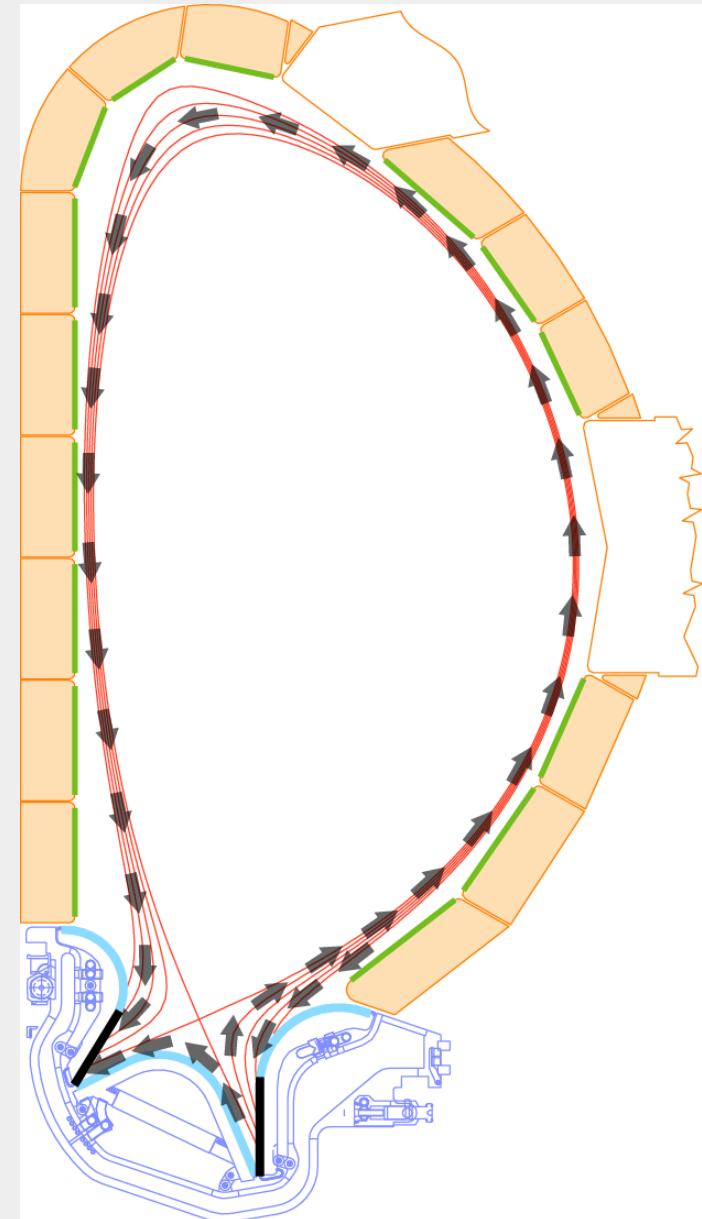
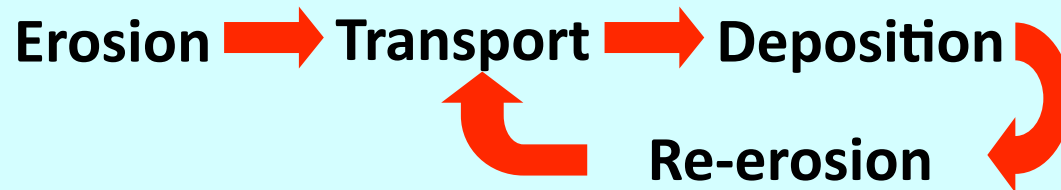
Summary and outlook

What are the basic ingredients of material migration?

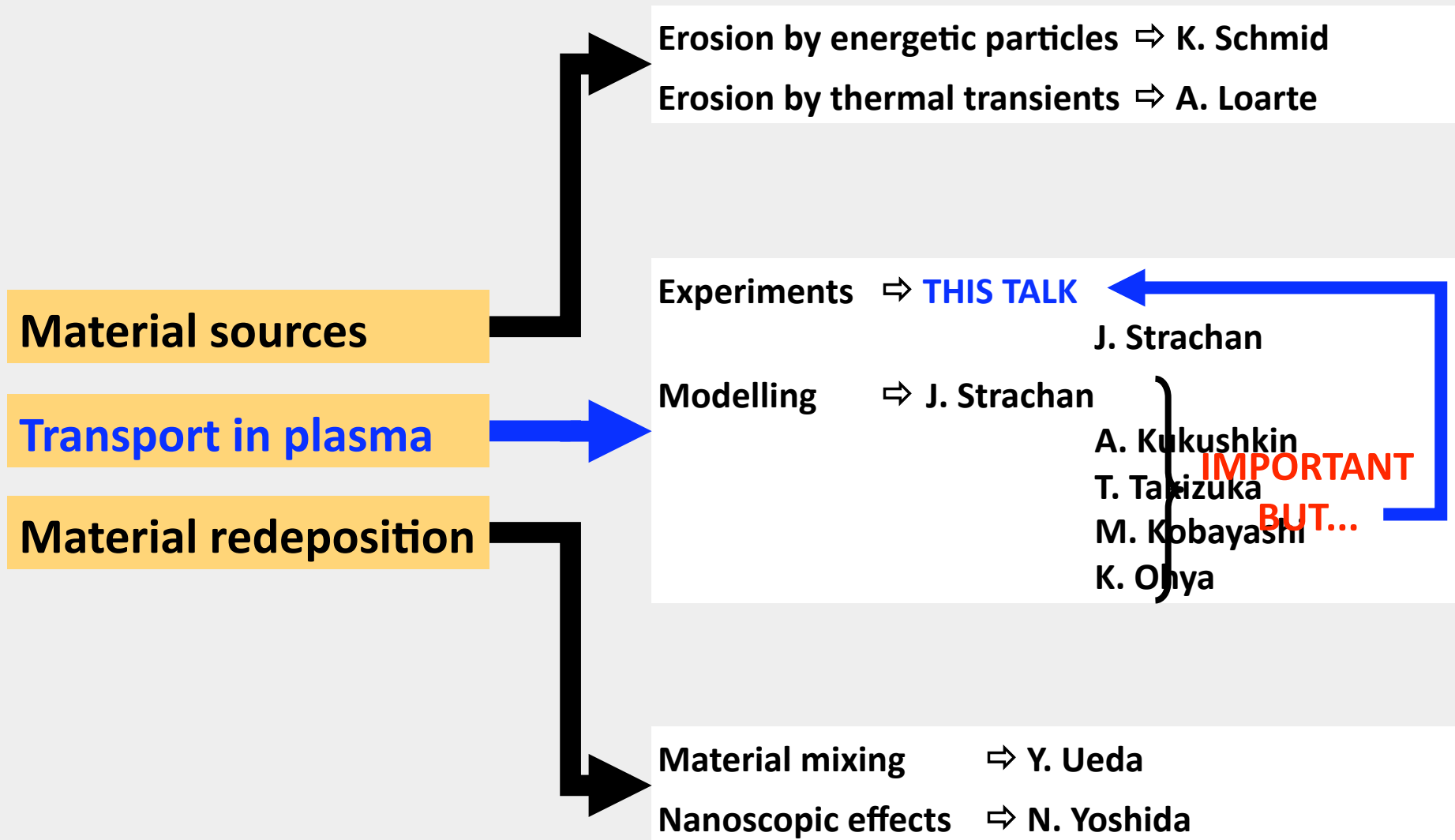
Plasma

Fuel ions + atoms (charge exchange) + impurity ions bombard 1st wall

Wall materials



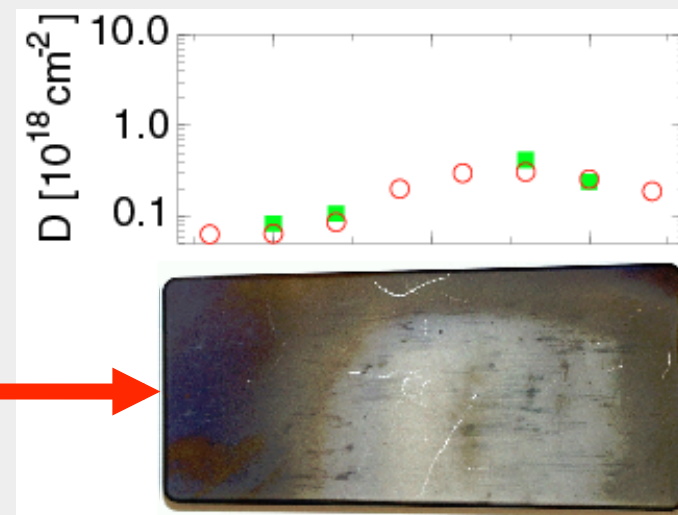
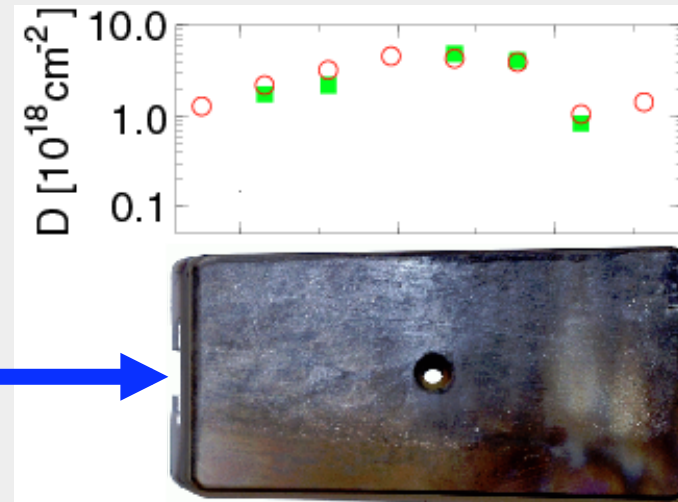
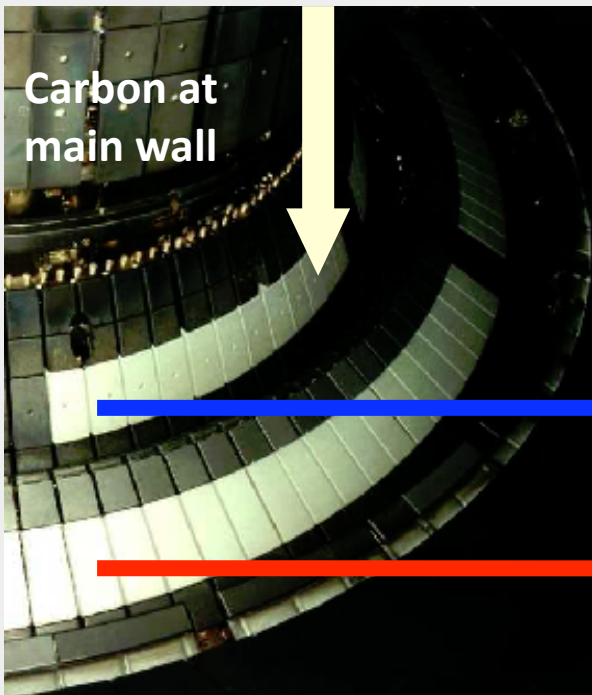
What's the connection to the other lectures?



What are the consequences of material migration?

Layer deposition and material mixing!

Freshly installed tungsten divertor in ASDEX Upgrade

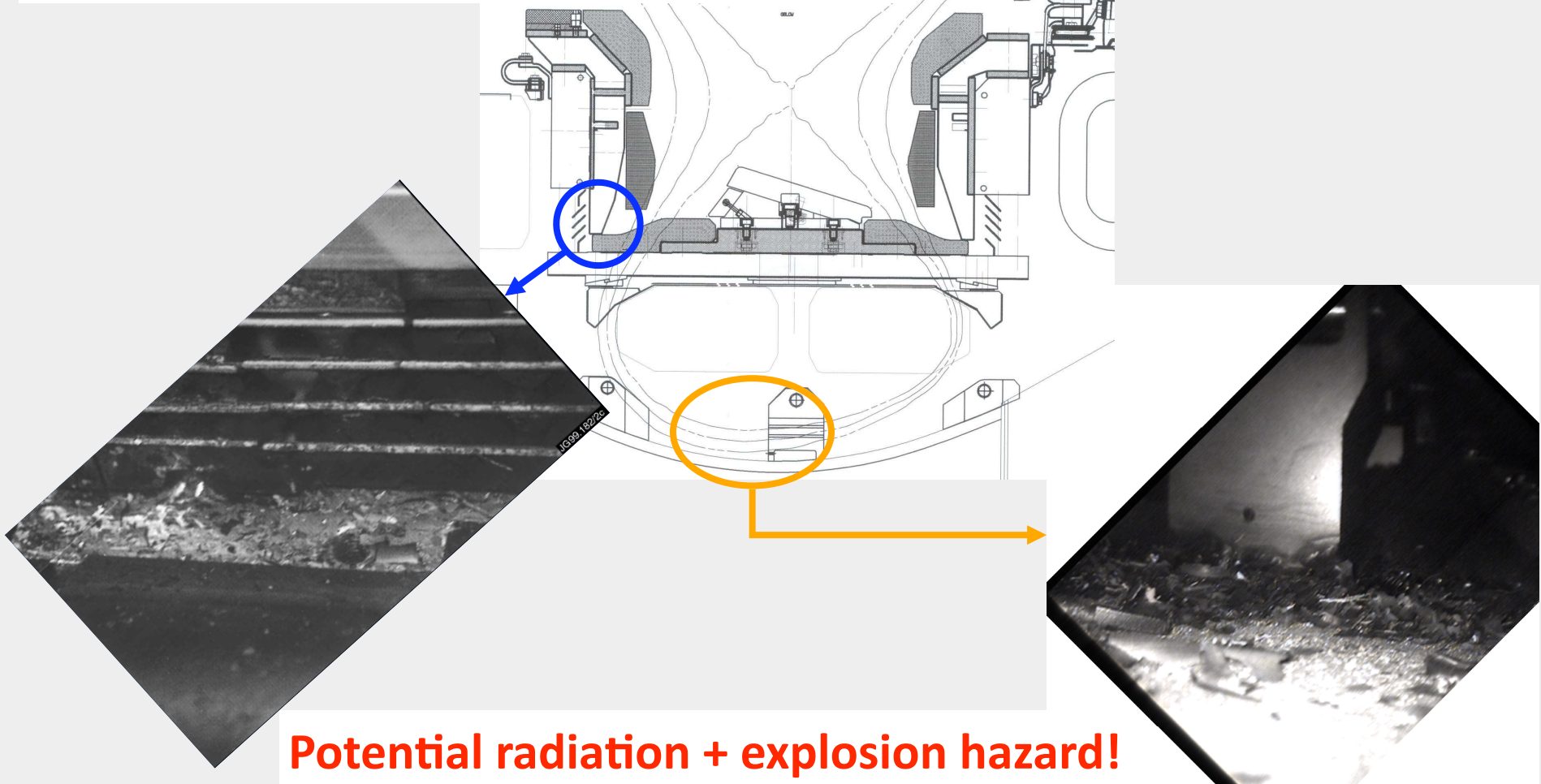


Deposited layers may form ever growing inventory of buried fuel!

What happens if deposited layers become too thick?

S. Brezinsek

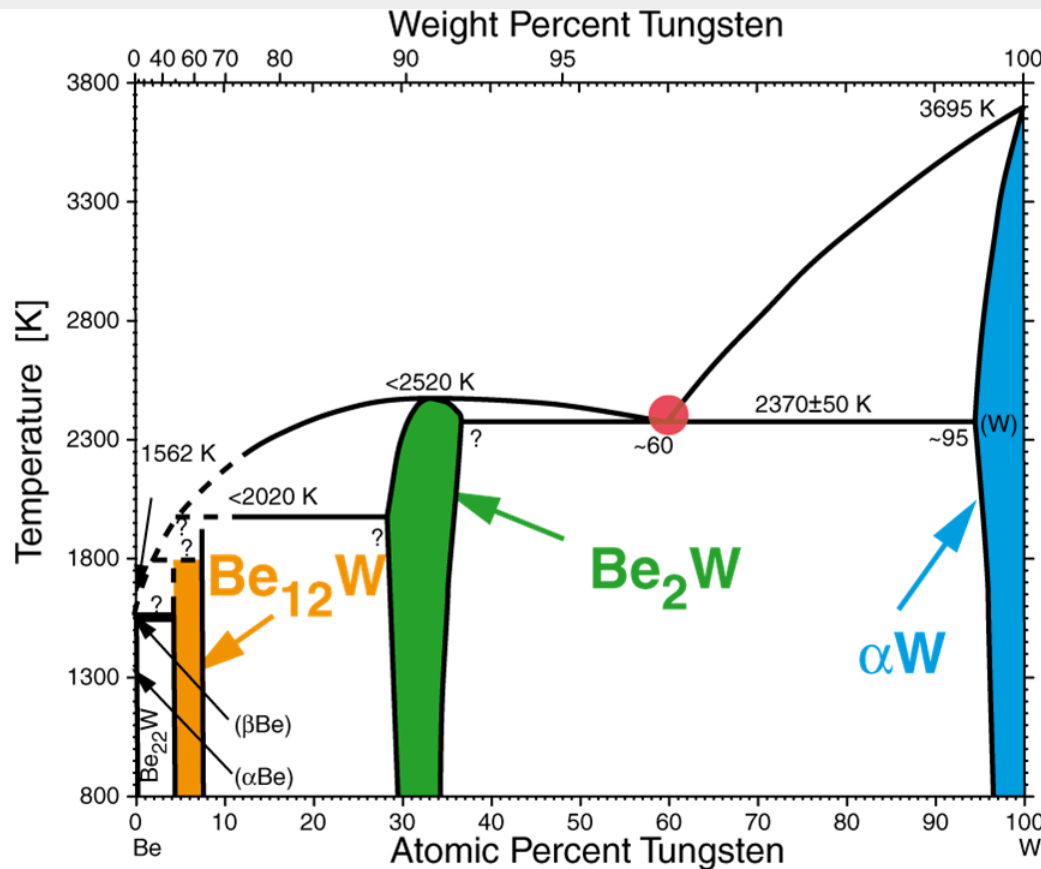
Layers delaminate and flake off, forming radioactive and chemically reactive dust



Negative consequences of material mixing?

YES! Example: beryllium and tungsten can form alloys

Ch. Linsmeier



melting point: 3695 K → 2370 K → 2520 K → ~1570 K
with increasing Be content

Overview and rationale

Material transport processes

Particle collisions

Plasma turbulence

Experiments

Phenomenological observations

Specific experiments

Summary and outlook

Key questions of material (impurity) transport

**For given impurity edge density,
what is the impurity density in the plasma centre?
or
What is the impurity residence time compared to
the fuel ion residence time in the plasma?**

Core transport coefficients

**For given material erosion source,
how much gets into the confined plasma?**

Screening factor, divertor retention

Where are eroded impurities re-deposited?

Migration paths

Impurity transport $\perp B$ by particle collisions

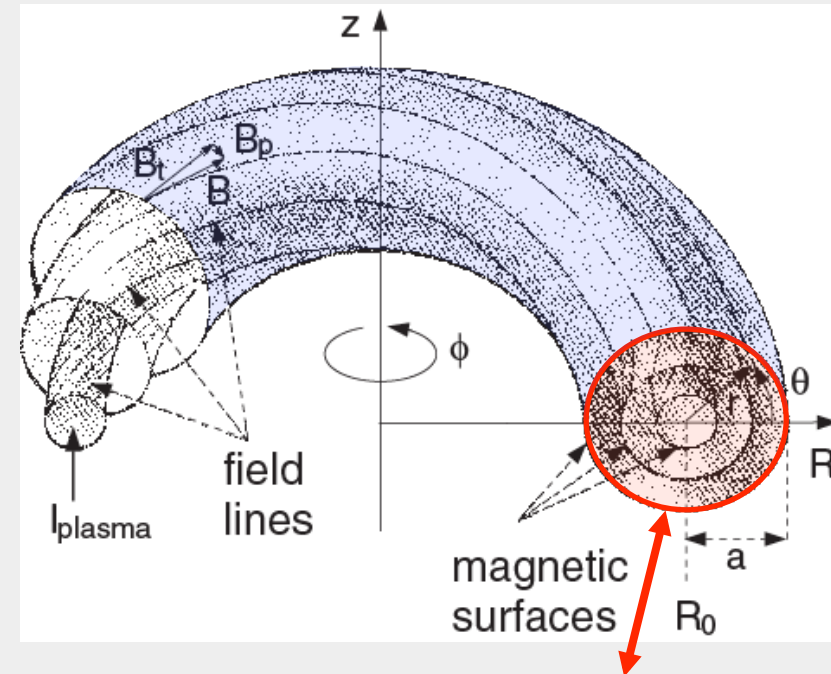
Particle conservation

$$\frac{\partial n_{I,Z}}{\partial t} = -\nabla \cdot \Gamma_{I,Z} + Q_{I,Z}$$

Ions bound to flux surface

$$\langle n_I \rangle = n_I$$

i.e. densities constant on flux surface



Impurity density is only a function of **flux surface label**

$$r = \sqrt{V / (2\pi^2 R_0)}$$

and flux is described by **diffusion** + **convection**

$$\frac{\partial n_{I,Z}}{\partial t} = \frac{1}{r} \frac{\partial}{\partial r} r \left(D^* \frac{\partial n_{I,Z}}{\partial r} - v^* n_{I,Z} \right) + Q_{I,Z}$$

Transport coefficients \Rightarrow averages over flux surface

Impurity transport \perp B by particle collisions

$$D = D^{CL} + D^{PS} + D^{BP}$$

$$D^{CL} \cong \frac{m_I kT v_{ID}}{B_0^2 e^2 Z^2} \propto \frac{1}{\sqrt{T} B_0^2 Z^2}$$

Classical transport
due to collisional friction forces \perp B

$$D^{PS} \cong 2q^2 D^{CL} \propto \frac{1}{\sqrt{T} B_p^2 Z^2}$$

Pfirsch-Schlüter transport
due to collisional friction forces \parallel B

$$D^{BP} \cong \frac{q^2}{\varepsilon^2} \frac{kT \mu_{ID}^*}{B_0^2 e^2 Z n_I} \propto \frac{1}{\sqrt{T} B_p^2 Z n_I}$$

Banana-Plateau transport
due to viscosity forces \parallel B

$$\varepsilon = \frac{r}{R_0}$$

$$q = \varepsilon \frac{B_T}{B_p}$$

Impurity transport \perp B by particle collisions

$$V = V^{CL} + V^{PS} + V^{BP}$$

$$V^{XX} = D^{XX} Z \left(\frac{d \ln n_D}{dr} + H^{XX} \frac{d \ln T}{dr} \right)$$

All drifts have the same form but the sign of H^{XX} may change!

Why is this important?

$$\frac{d \ln n_Z}{dr} = Z \frac{d \ln n_I}{dr} \left(1 + H_{eff} \frac{d \ln T}{dr} / \frac{d \ln n_I}{dr} \right)$$



Temperature screening factor \Rightarrow generally negative!

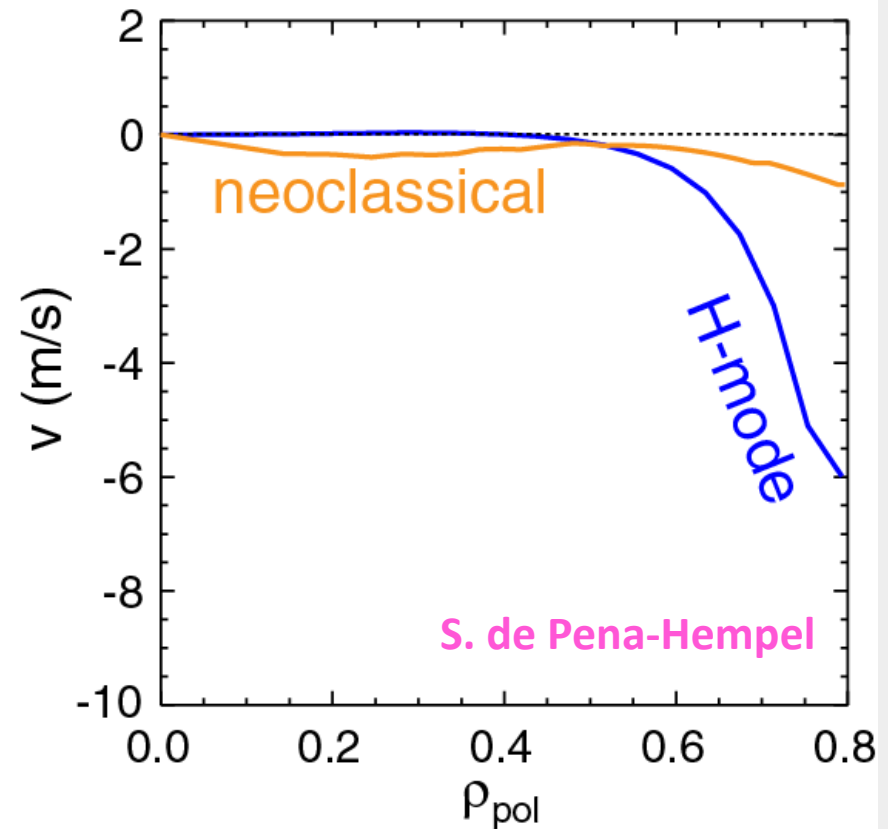
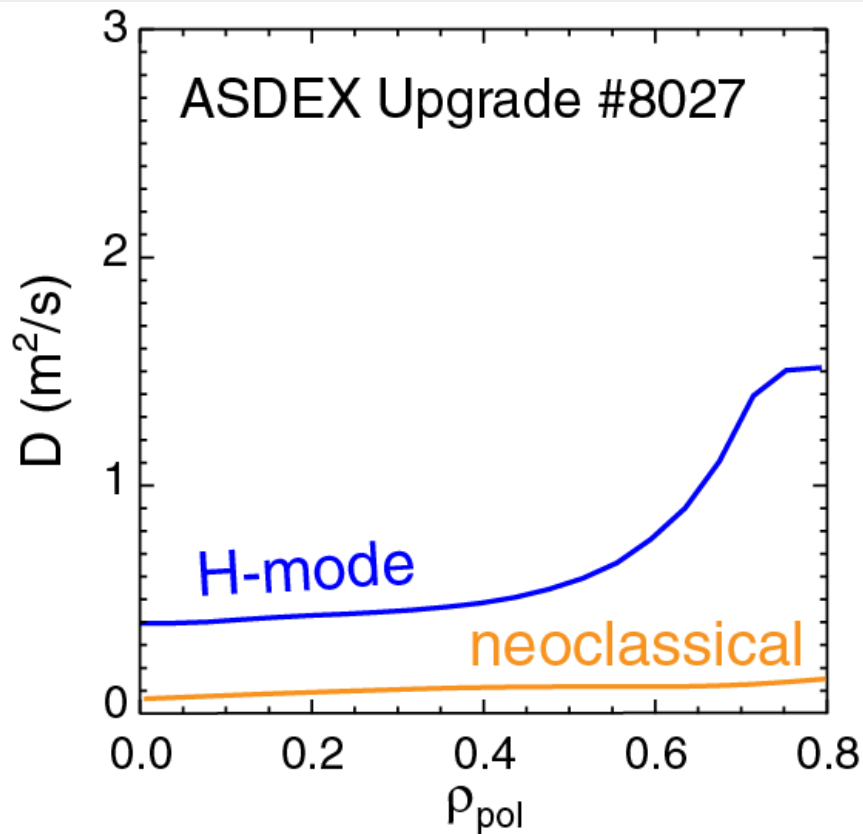
Pure neoclassical transport
leads to central impurity peaking

Peaked temperature profile
alleviates problem

Is transport really only due to collisions?

Measure $n_z(r,t)$ after transient applied disturbance

⇒ $D(r)$ and $v(r)$



NO: "Anomalous diffusion" generally much larger!

Is "anomalous" transport good or bad?

Recall expression for impurity profile shape:

$$\frac{d \ln n_Z}{dr} = Z \frac{d \ln n_I}{dr} \left(1 + H_{eff} \frac{d \ln T}{dr} / \frac{d \ln n_I}{dr} \right) \left(\frac{D}{D + D_{AN}} \right)$$

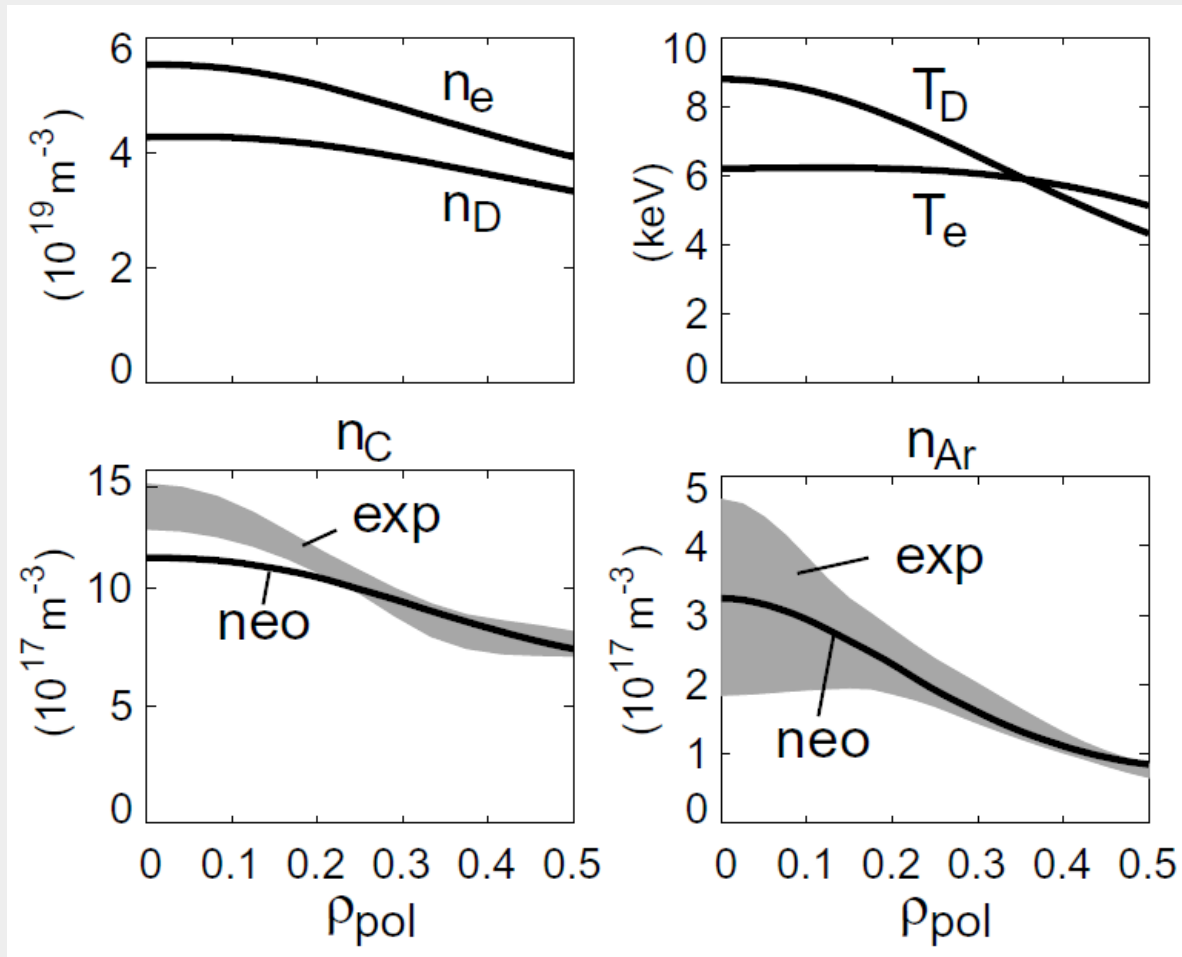
GOOD! D_{AN} decreases impurity profile peaking

Also holds for fuel ions so that $d \ln n_I / dr \searrow$

Purely collisional transport

Discharge with quiescent plasma

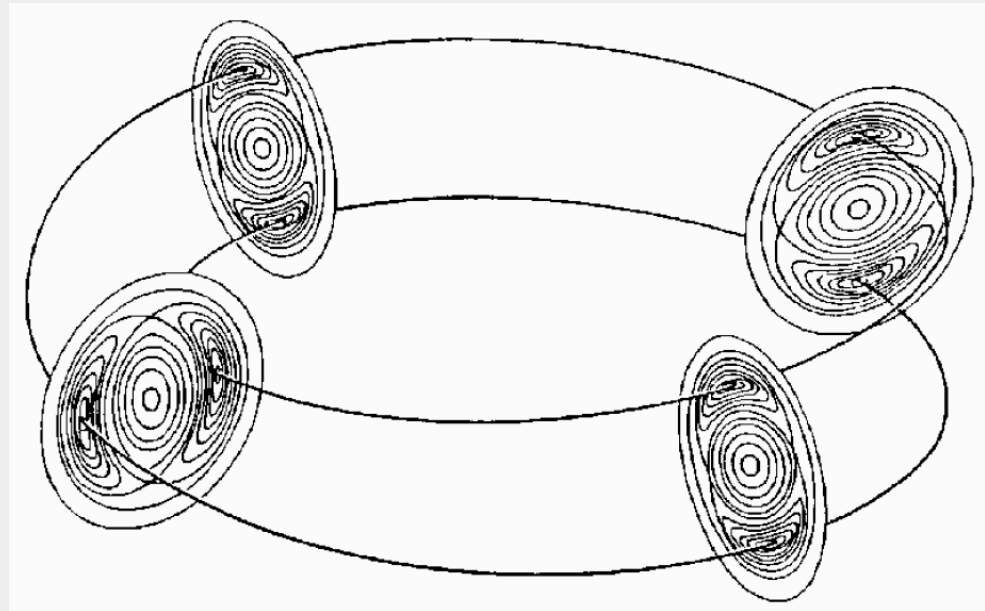
R. Dux



Impurity peaking in centre according to neoclassical D and ν

What are the origins of "anomalous" transport?

Large scale MHD instabilities
create radial "shortcut"



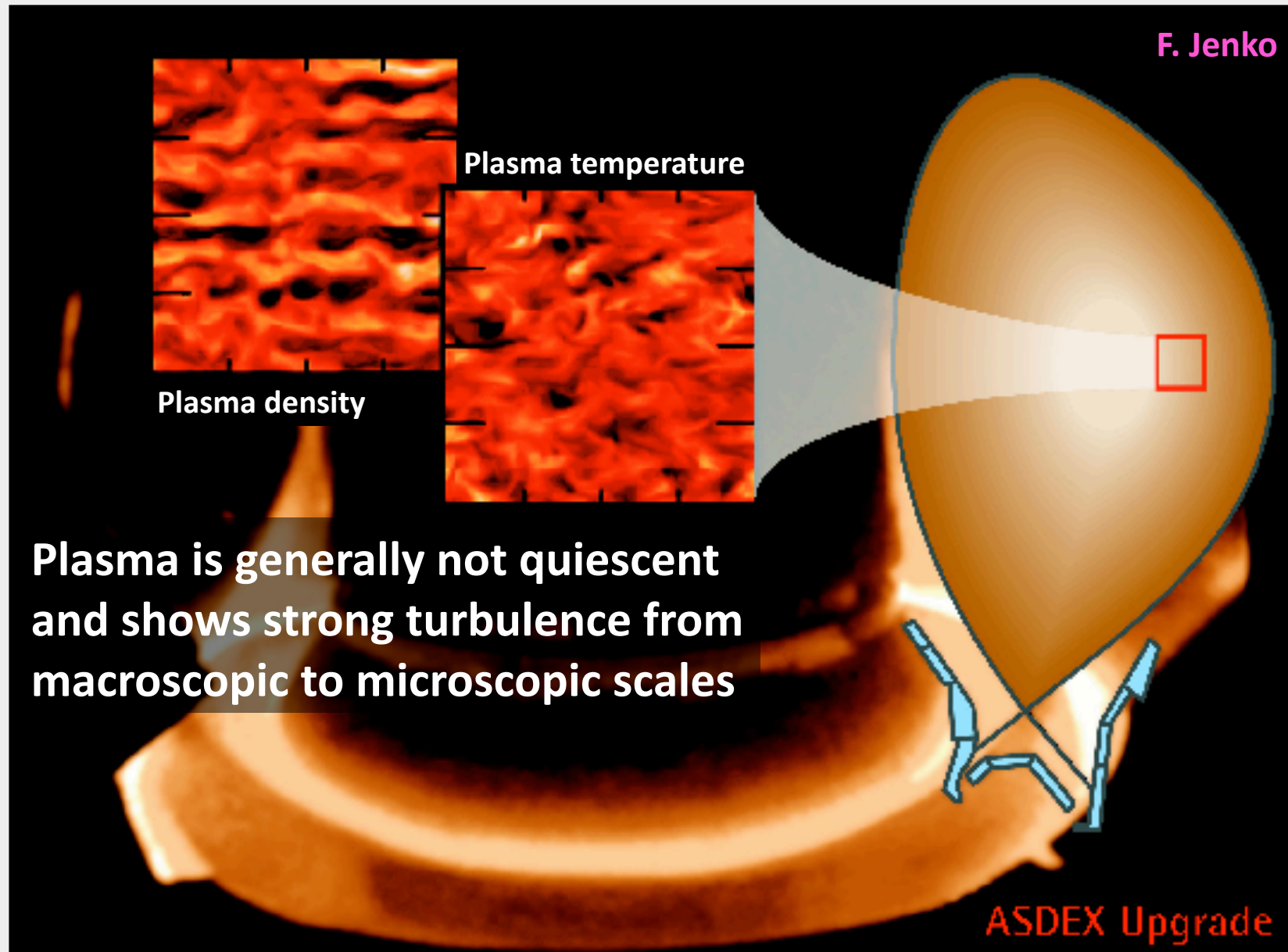
Not the whole story:

Anomalous diffusion shows also in absence of MHD instabilities



Turbulence, carrying impurities with it!

Turbulent processes in a Tokamak plasma?



How can plasma turbulence be described?

F. Jenko

Ab initio model of plasma microturbulence
 \Rightarrow nonlinear gyrokinetic theory

Hot fusion plasmas are almost collisionless (even in the edge!)

Vlasov-Maxwell equations
 (self-consistent, nonlinear problem)

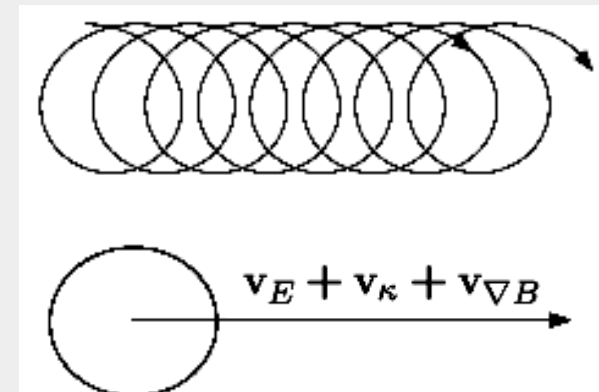
$$\left[\frac{\partial}{\partial t} + \mathbf{v} \cdot \frac{\partial}{\partial \mathbf{x}} + \frac{q}{m} \left(\mathbf{E} + \frac{\mathbf{v}}{c} \times \mathbf{B} \right) \cdot \frac{\partial}{\partial \mathbf{v}} \right] f(\mathbf{x}, \mathbf{v}, t) = 0$$

Eliminating the fast gyromotion...

[Frieman, Chen, Lee, Hahm, Brizard *et al.* in the 1980s]

$$\omega \ll \Omega$$

Charged rings as quasiparticles; important kinetic effects retained non-perturbatively!



\Rightarrow Irrelevant (small) spatio-temporal scales are removed!

The nonlinear gyrokinetic equations

$$f = f(\mathbf{X}, v_{\parallel}, \mu; t)$$

advection equation/conservation law

$$\frac{\partial f}{\partial t} + \dot{\mathbf{X}} \cdot \frac{\partial f}{\partial \mathbf{X}} + \dot{v}_{\parallel} \frac{\partial f}{\partial v_{\parallel}} = 0$$

$$\dot{\mathbf{X}} = v_{\parallel} \mathbf{b} + \frac{B}{B_{\parallel}^*} \left(\frac{v_{\parallel}}{B} \bar{\mathbf{B}}_{1\perp} + \mathbf{v}_{\perp} \right)$$

$$\mathbf{v}_{\perp} \equiv \frac{c}{B^2} \bar{\mathbf{E}}_1 \times \mathbf{B} + \frac{\mu}{m\Omega} \mathbf{b} \times \nabla (B + \bar{B}_{1\parallel}) + \frac{v_{\parallel}^2}{\Omega} (\nabla \times \mathbf{b})_{\perp}$$

$$\dot{v}_{\parallel} = \frac{\dot{\mathbf{X}}}{mv_{\parallel}} \cdot (e\bar{\mathbf{E}}_1 - \mu \nabla (B + \bar{B}_{1\parallel}))$$

\mathbf{X} = position of the gyrocenter

v_{\parallel} = parallel velocity

μ = magnetic moment

F. Jenko

Corresponding field equations

$$\frac{n_1}{n_0} = \frac{\bar{n}_1}{n_0} - (1 - \|I_0^2\|) \frac{e\phi_1}{T} + \|x I_0 I_1\| \frac{B_{1\parallel}}{B}$$

$$\nabla_{\perp}^2 A_{1\parallel} = -\frac{4\pi}{c} \sum \bar{J}_{1\parallel}$$

$$\frac{B_{1\parallel}}{B} = -\sum \epsilon_{\beta} \left(\frac{\bar{p}_{1\perp}}{n_0 T} + \|x I_1 I_0\| \frac{e\phi_1}{T} + \|x^2 I_1^2\| \frac{B_{1\parallel}}{B} \right)$$

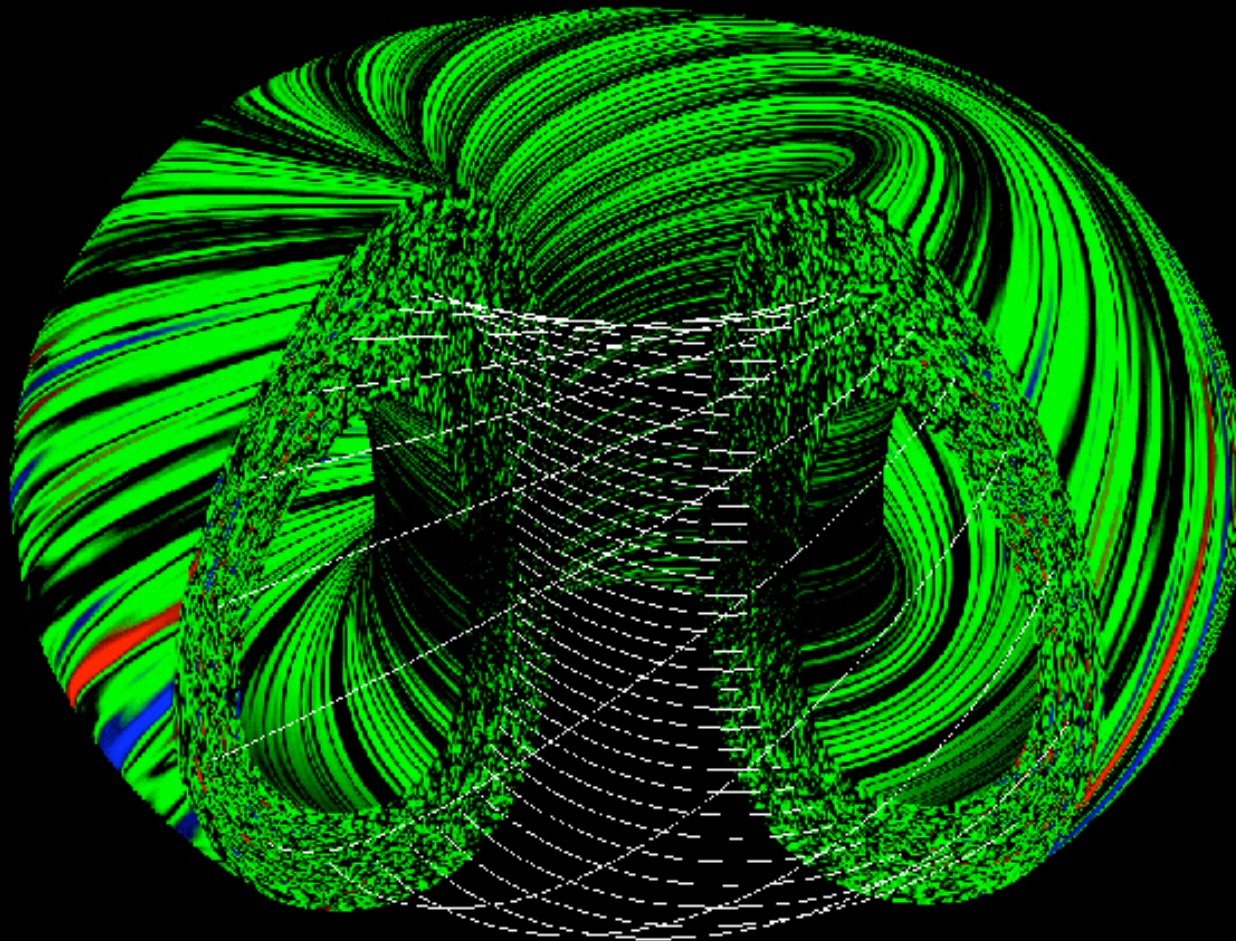
Nonlinear integro-differential equations in 3+2 dimensions

Progress only recently due to complexity of the system

Plasma turbulence is quasi-two-dimensional



Work with flux tubes, using field-aligned coordinates

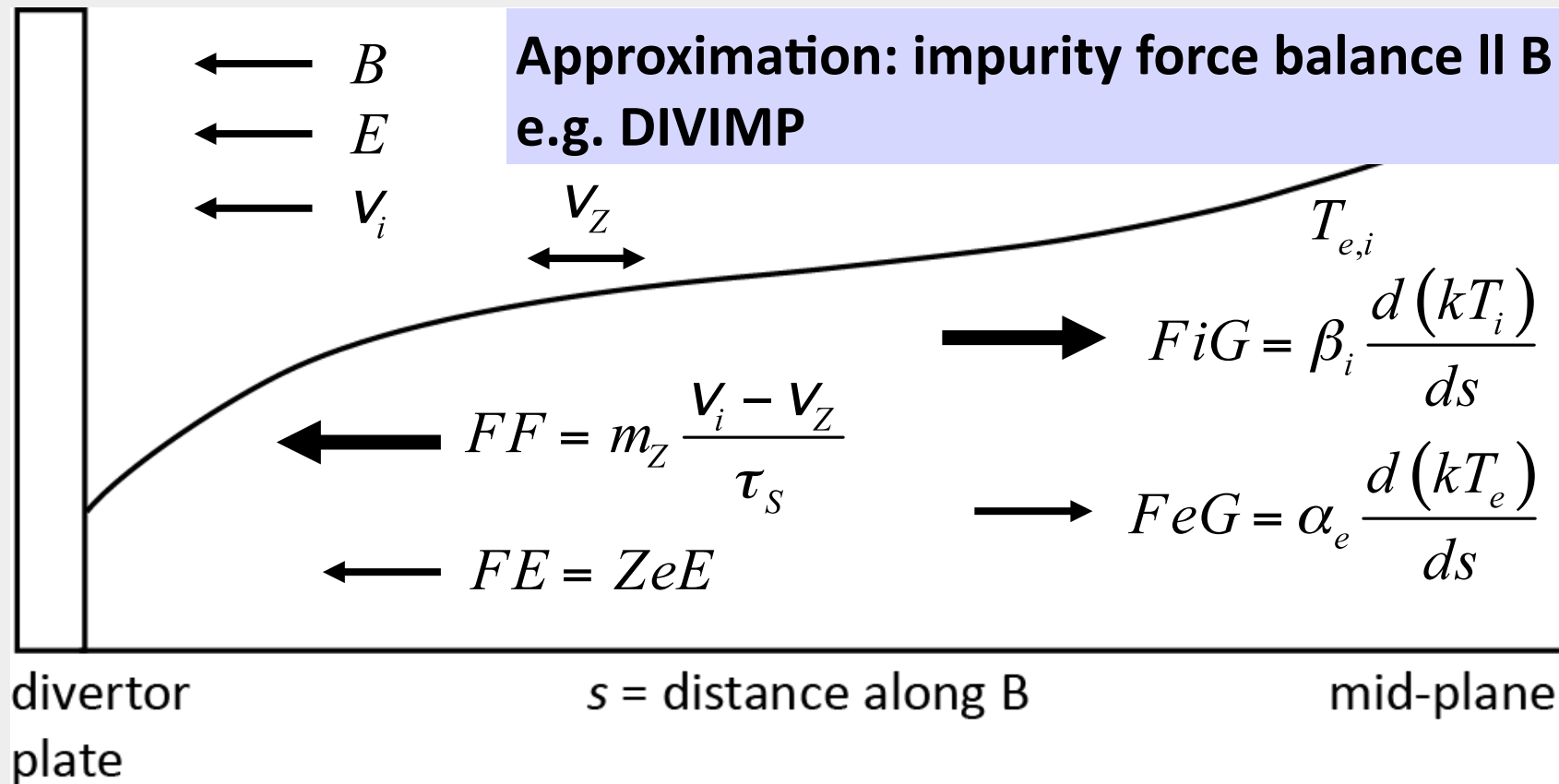


Still requires $O(100000)$ CPU-hours!

F. Jenko

Impurity transport in SOL

B-field intersects material surface \Rightarrow transport \parallel B becomes important!



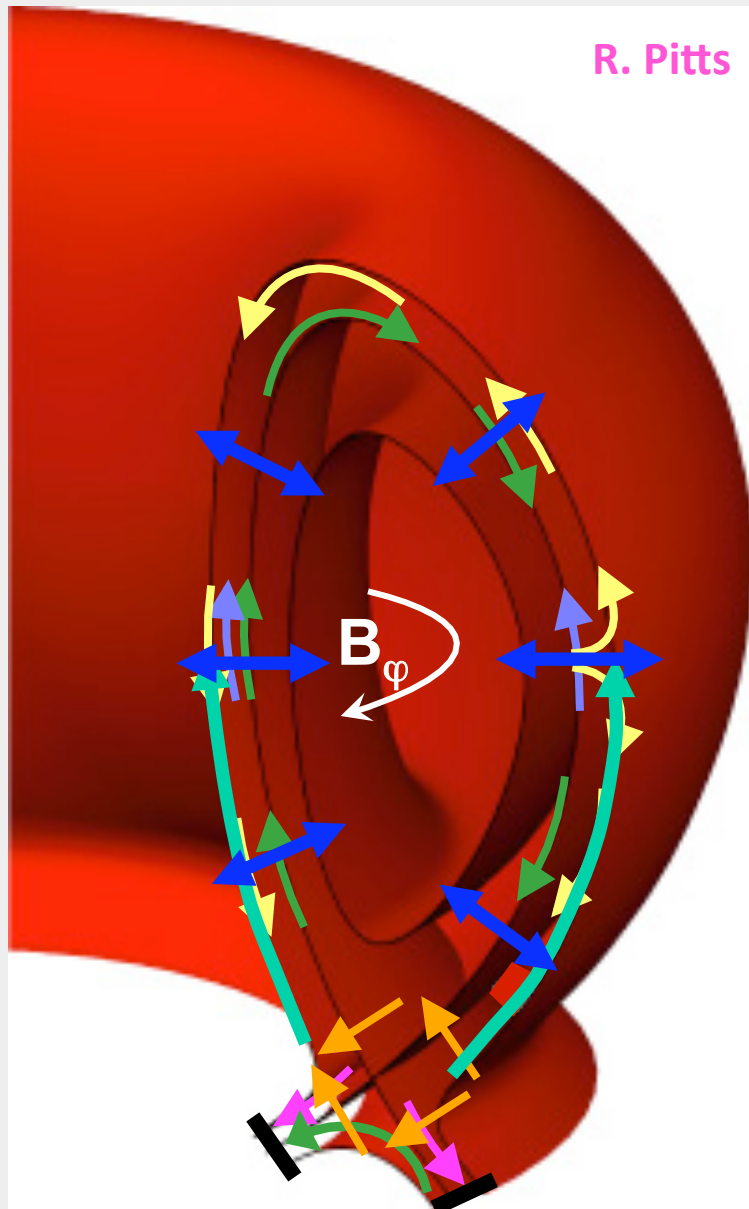
$$F_Z = -\frac{1}{n_Z} \frac{dp_Z}{ds} + FF + FE + FiG + FeG + \dots$$

$$\tau_s \propto m_Z \frac{T_i^{3/2}}{n_i Z^2}$$

$$\alpha_e \cong 0.71 Z^2$$

$$\beta_i \cong 2.65 Z^2$$

Is that the whole story?



Diffusion and convection $\perp B$



T gradients $\parallel B$



NO: drifts & flows

$E_r \times B, \nabla p \times B$	
$E_\theta \times B$	
Pfirsch-Schlüter	
Ballooning	
Divertor sink	

How to improve the quasi 1D-model?

Kinetic equations → Moments of ion and electron distribution functions → Fluid equations (Braginskii)

Particle balance

Momentum balance

Diffusion

Electron energy balance

Ion energy balance

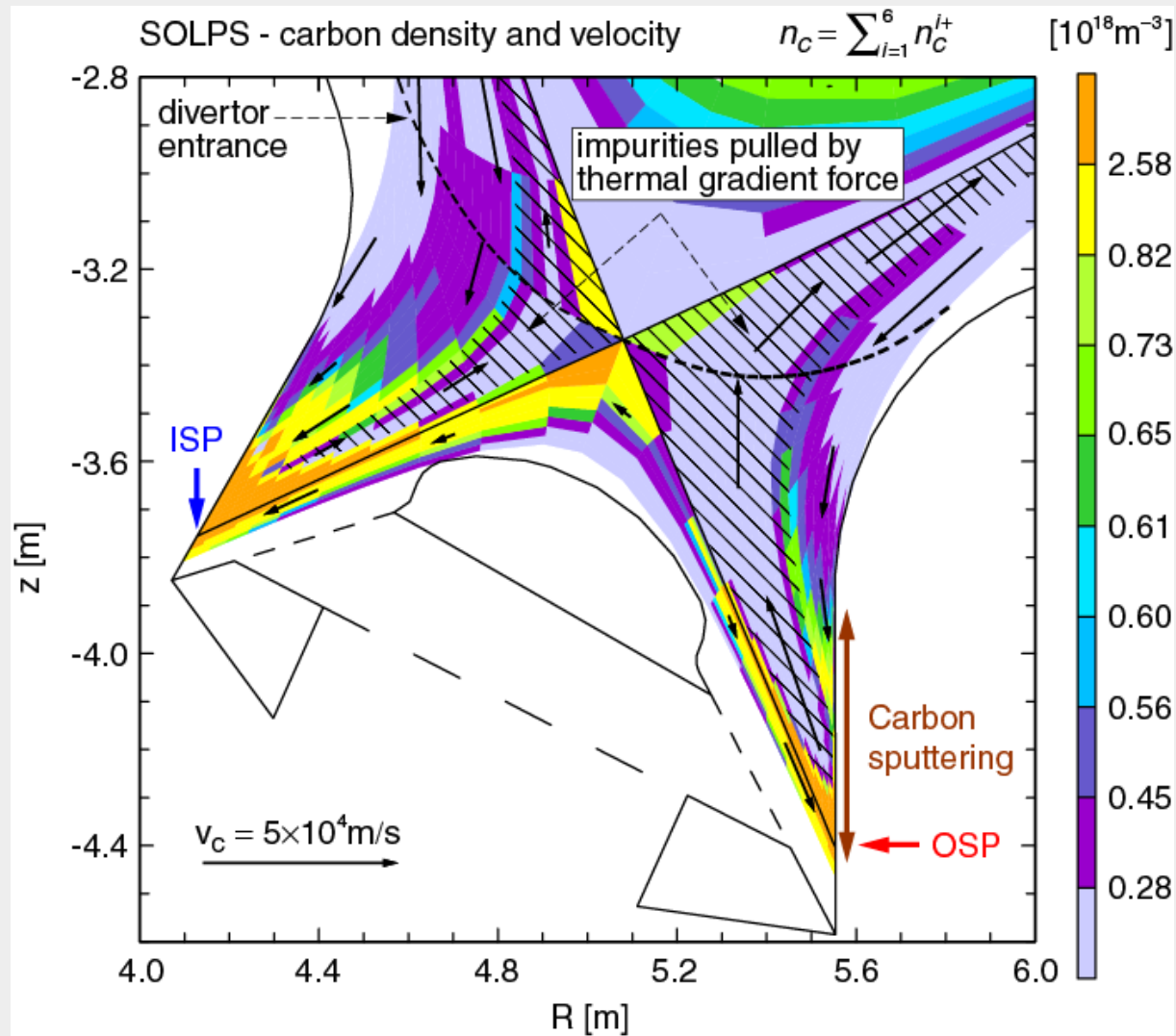
PLUS

Kinetic correction terms
(flux limiters)

Self consistent treatment of recycling
by iterative coupling to neutral transport code

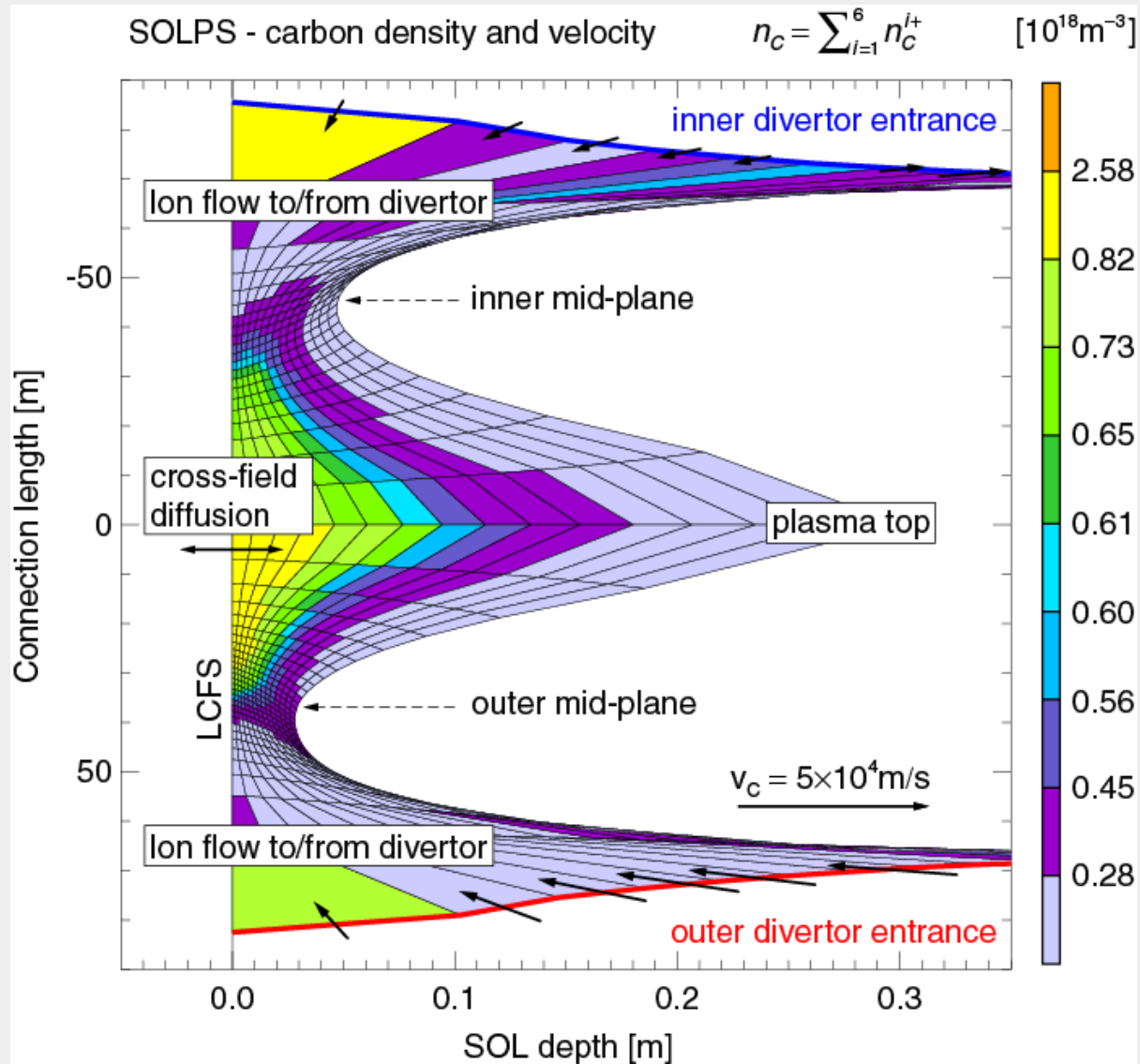
Standard used for ITER: B2-EIRENE

Example solution for ITER plasma



Data from
A. Kukushkin

Example solution for ITER plasma



Data from
A. Kukushkin

Challenge with experimental data

Overview and rationale

Material transport processes

Particle collisions

Plasma turbulence

Experiments

Phenomenological observations

Specific experiments

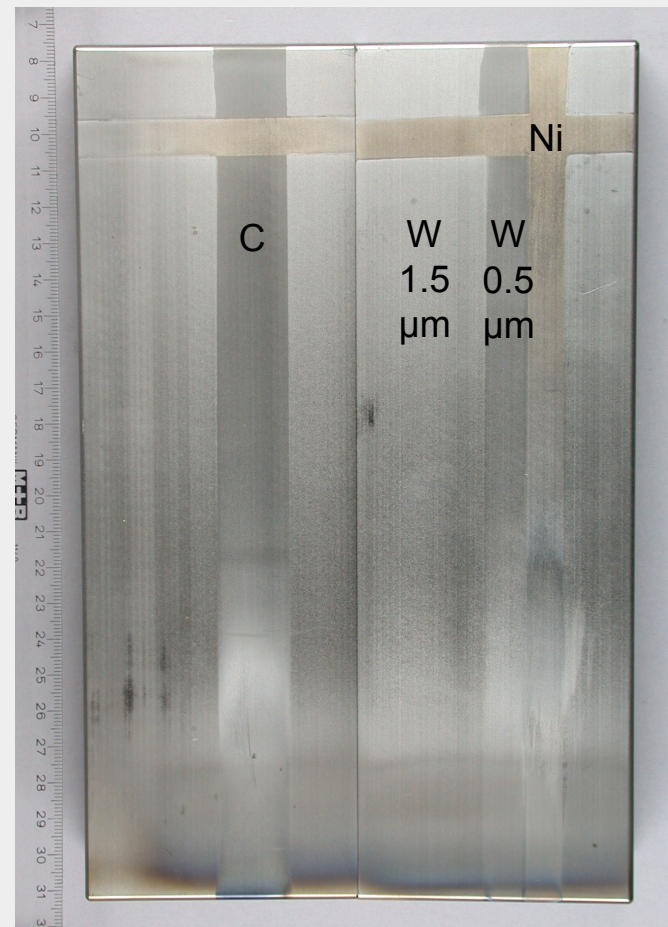
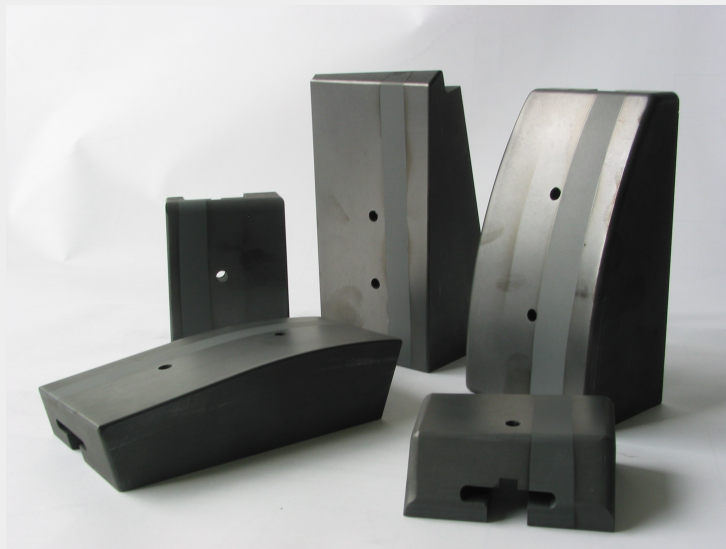
Summary and outlook

**Quantify material erosion and redeposition
by ex-situ surface analysis of retrieved wall tiles
and/or long term probes**

Identification of erosion and deposition dominated areas

Identification of net material migration balance

Example: ASDEX Upgrade - marker tiles

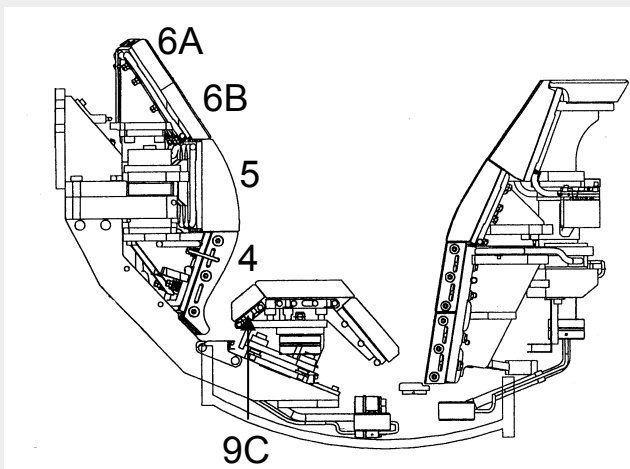
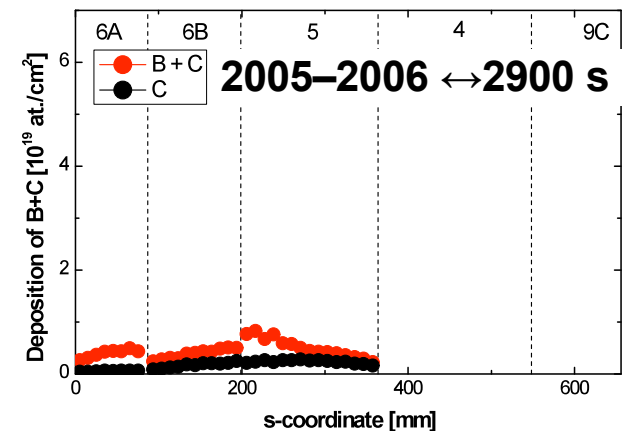
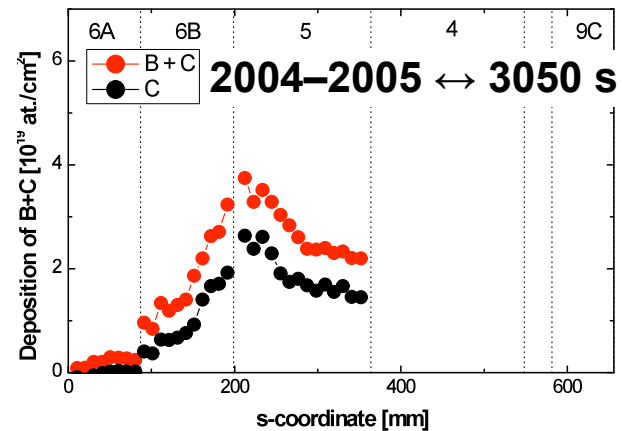
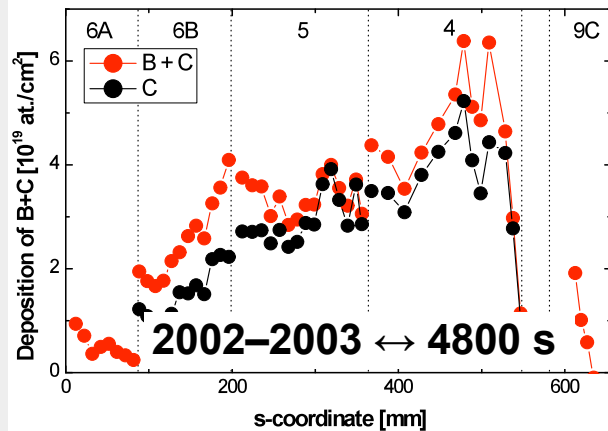


M. Mayer

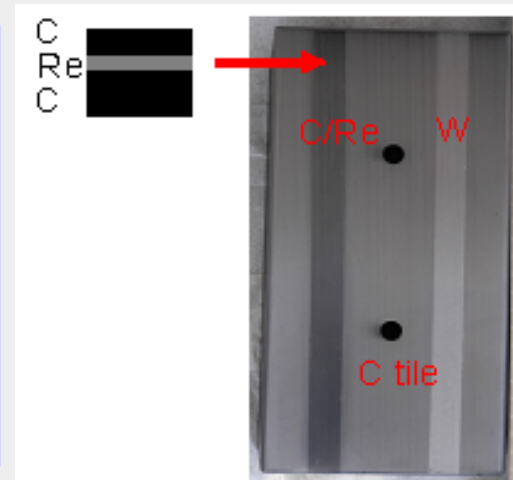
Example: ASDEX Upgrade - marker tiles

Carbon deposition in the inner divertor of ASDEX Upgrade

M. Mayer



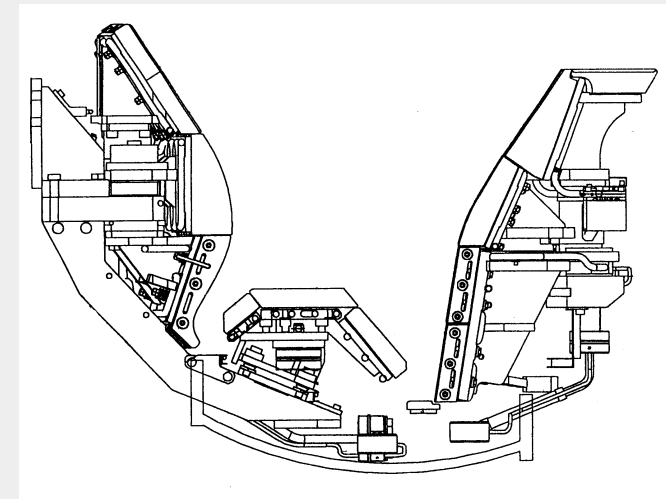
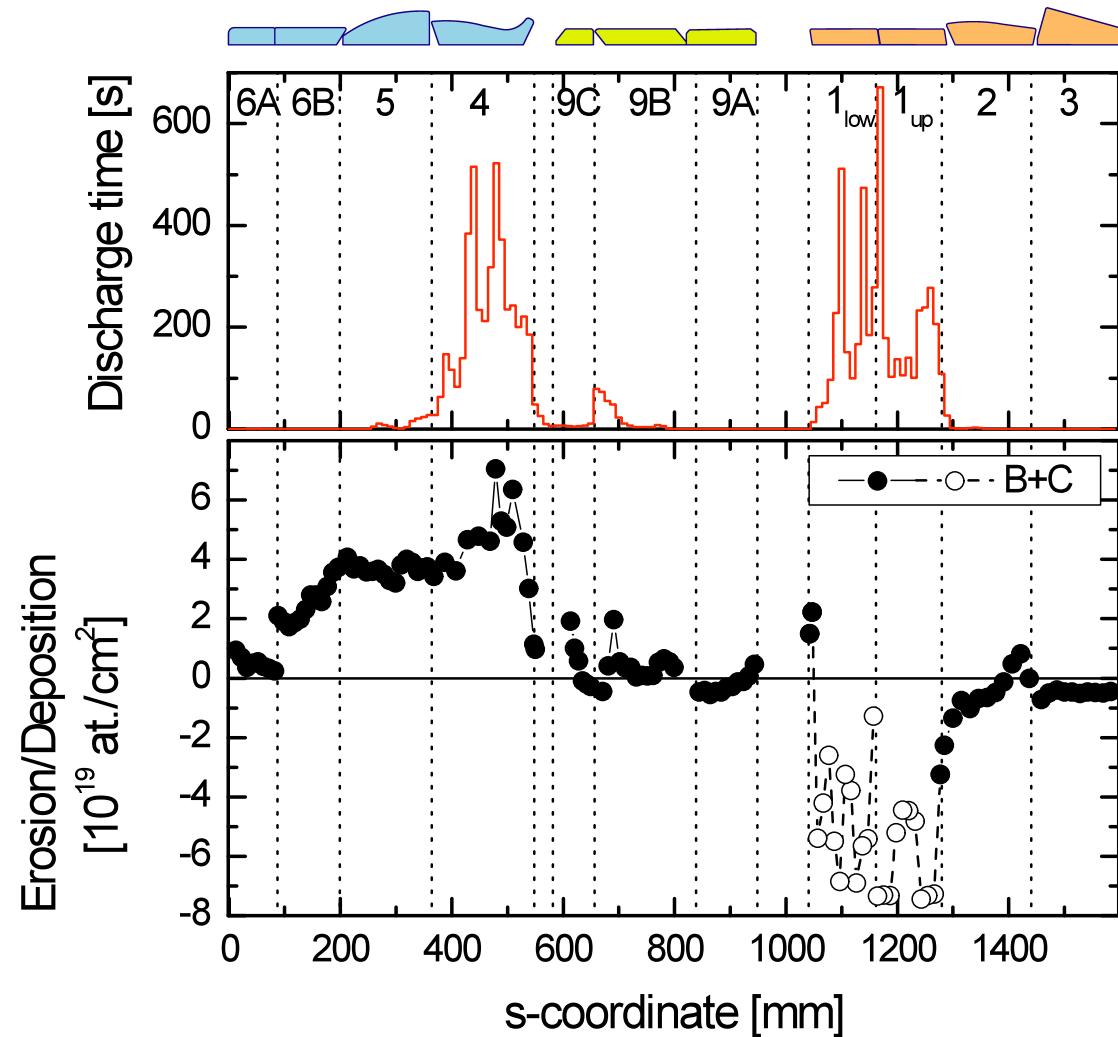
- Decrease of C-deposition on divertor tiles by factor 7 after W coverage of outer limiters
 - No change in outer divertor erosion
- ⇒ **Outboard limiters identified as main carbon source**



Example: ASDEX Upgrade - marker tiles

Carbon deposition / erosion in lower divertor of ASDEX Upgrade

M. Mayer

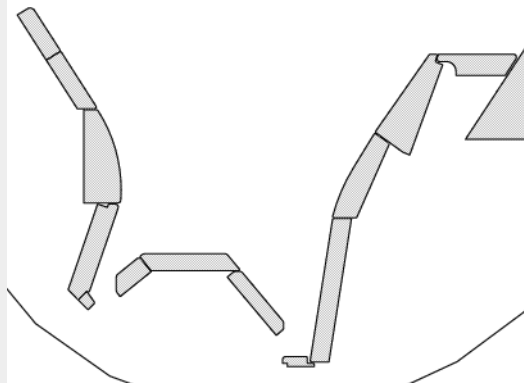


Deposition in
inner divertor
Erosion in
outer divertor

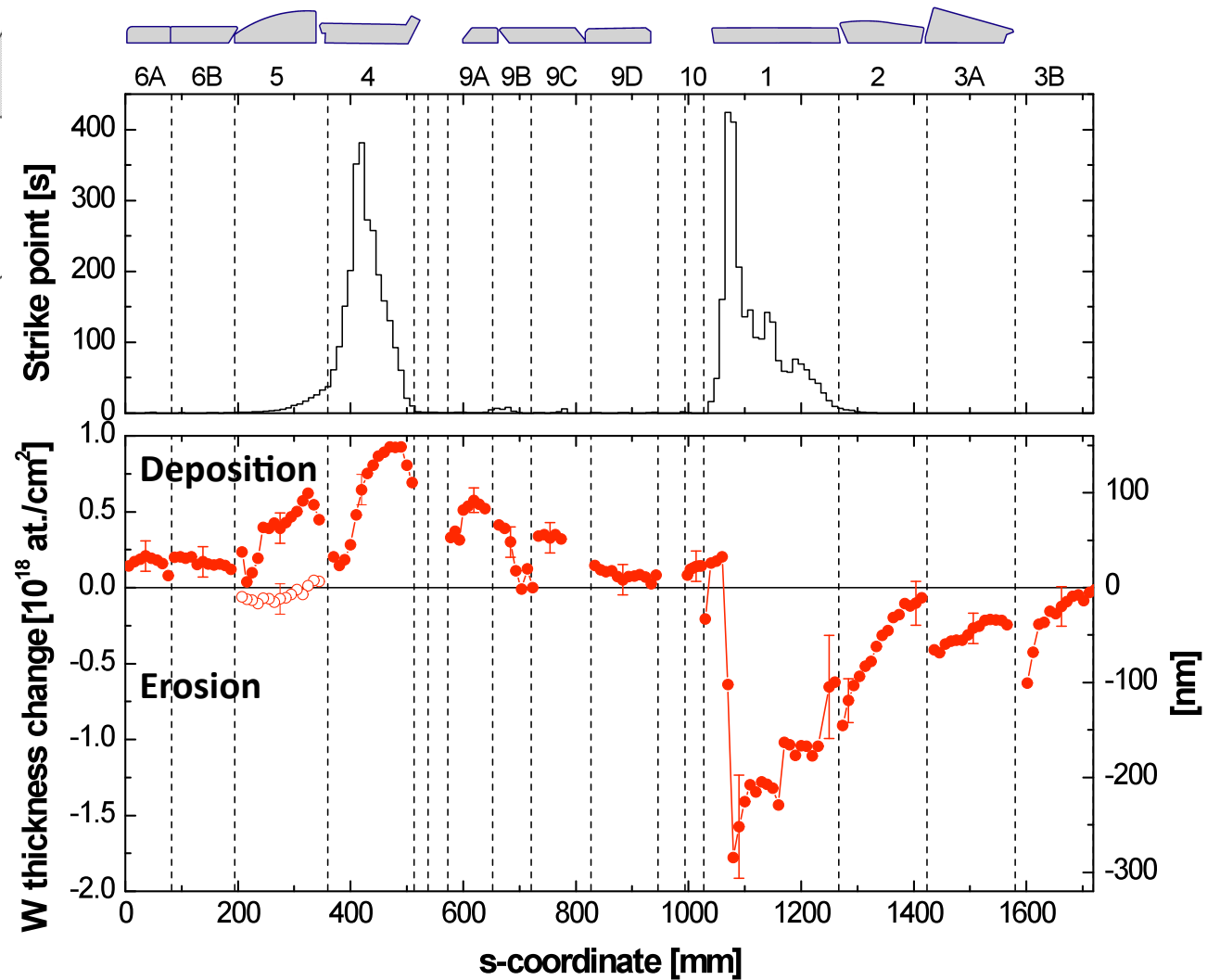
Example: ASDEX Upgrade - marker tiles



Tungsten deposition / erosion in lower divertor of ASDEX Upgrade

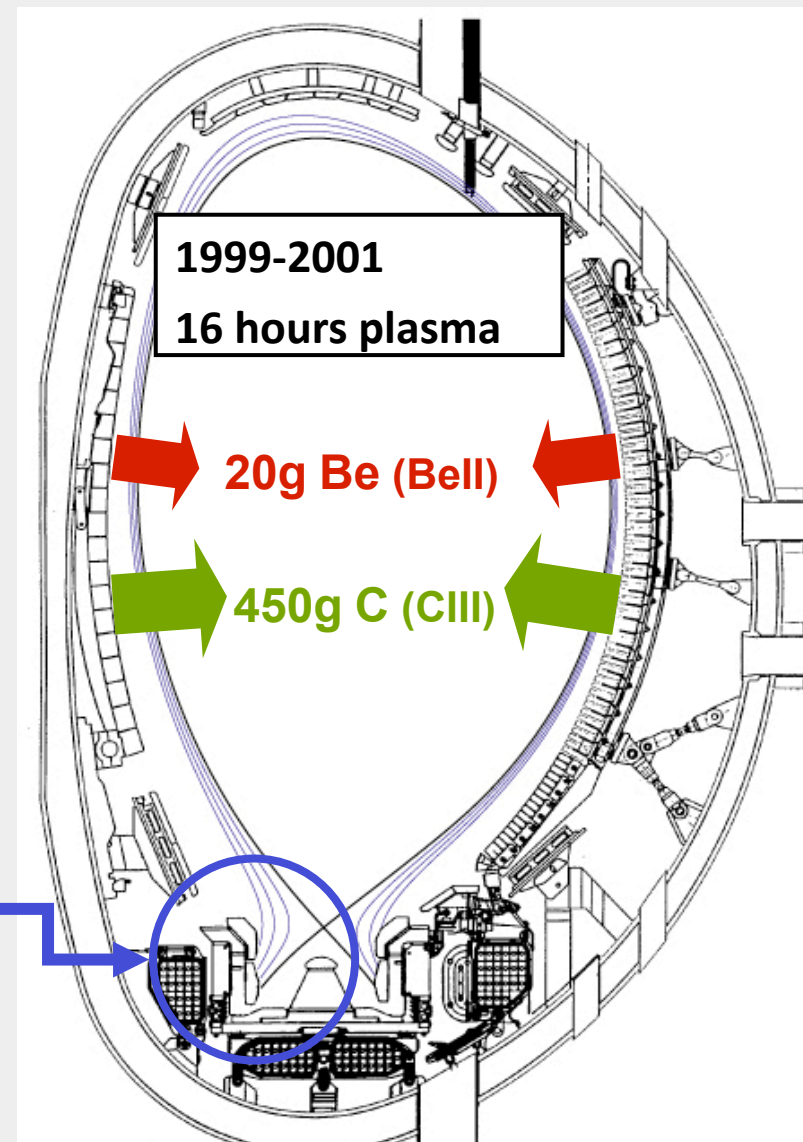
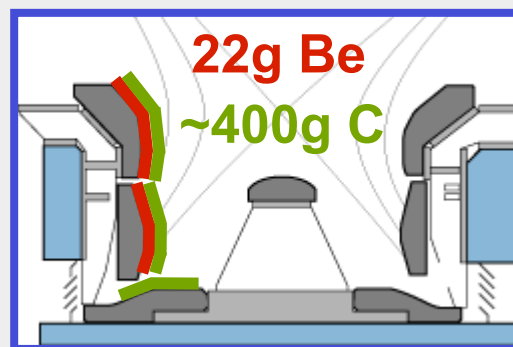


Deposition in inner divertor
Erosion in outer divertor



Example: JET accounting of Be & C erosion / deposition

- Spectroscopy + modelling
⇒ integral erosion flux
- Post mortem surface analysis
⇒ re-deposition → all at inner divertor



Likonen et al, JNM 337-339 (2005) 60, Matthews et al., EPS 2003

Advantages:

Independent of experiment programme

Possible to survey large vessel areas

Disadvantages:

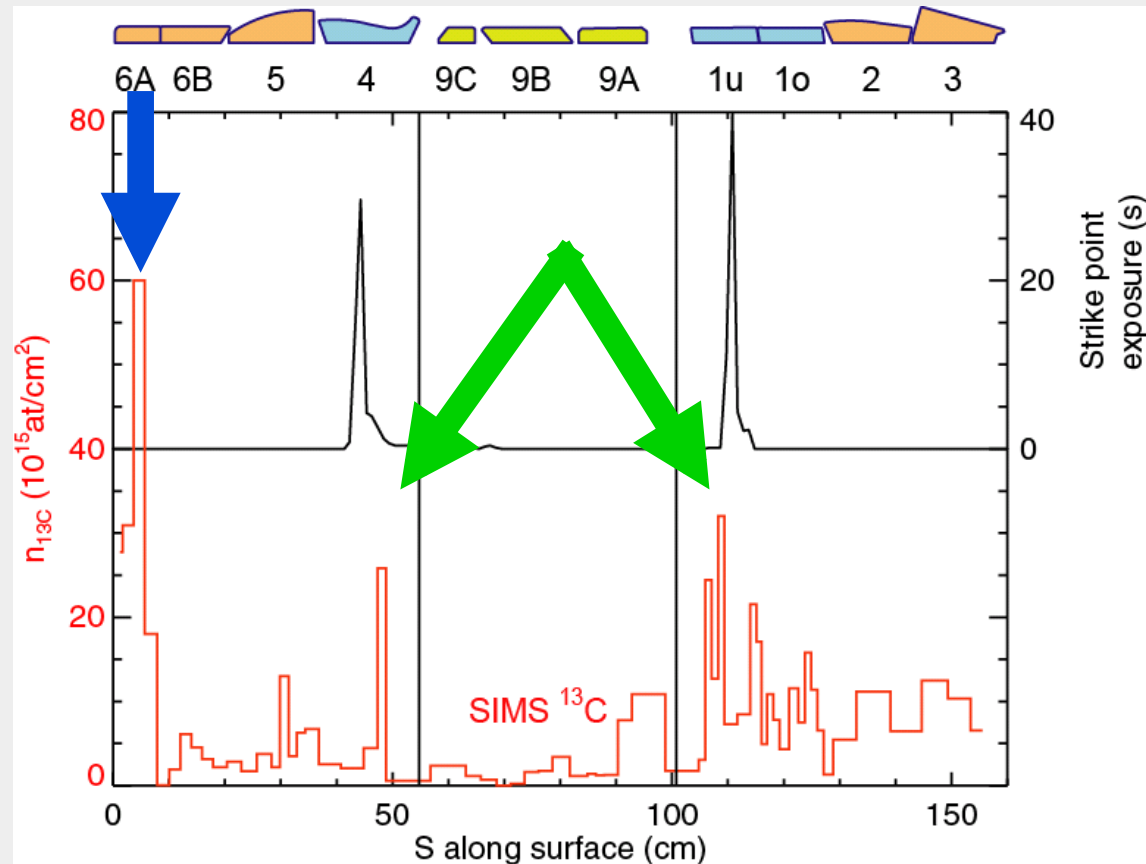
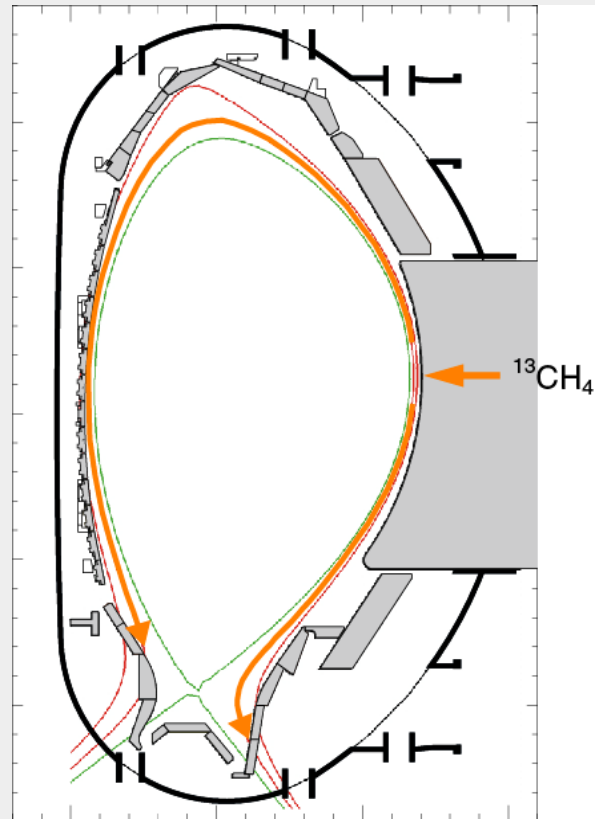
Integral over many plasma scenarios makes interpretation and code benchmarking difficult

Inject tracer material in discharges at the end of an experimental campaign

Quantify tracer deposition by ex-situ surface analysis of retrieved wall tiles and/or long term probes

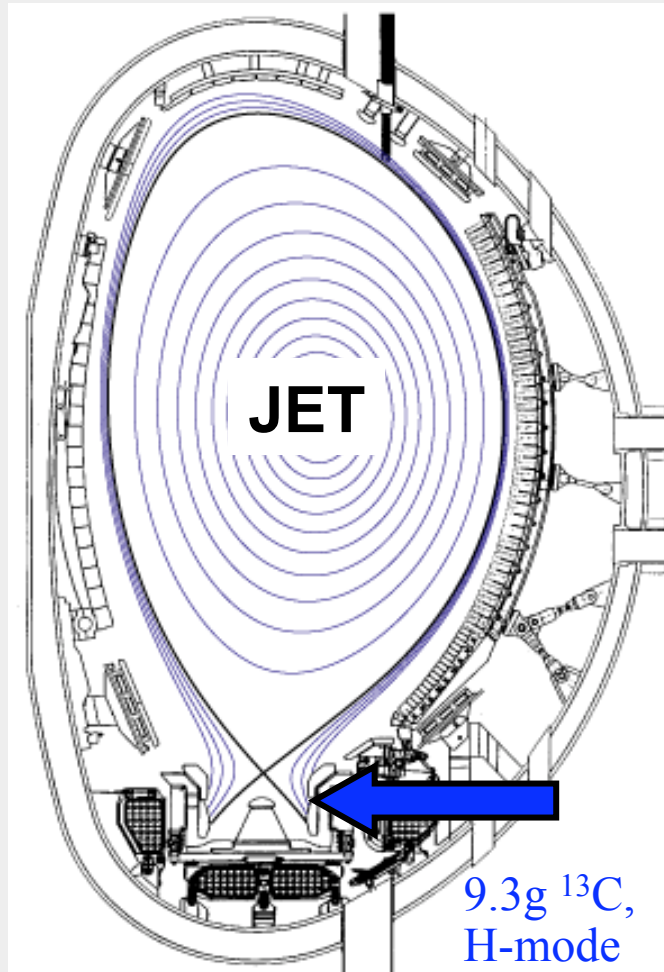
Identification of net material migration path (locally or globally) for particular discharge scenario

Example: $^{13}\text{CH}_4$ injection in ASDEX Upgrade



Observed deposition pattern determined by both **plasma flow** and by **geometry**

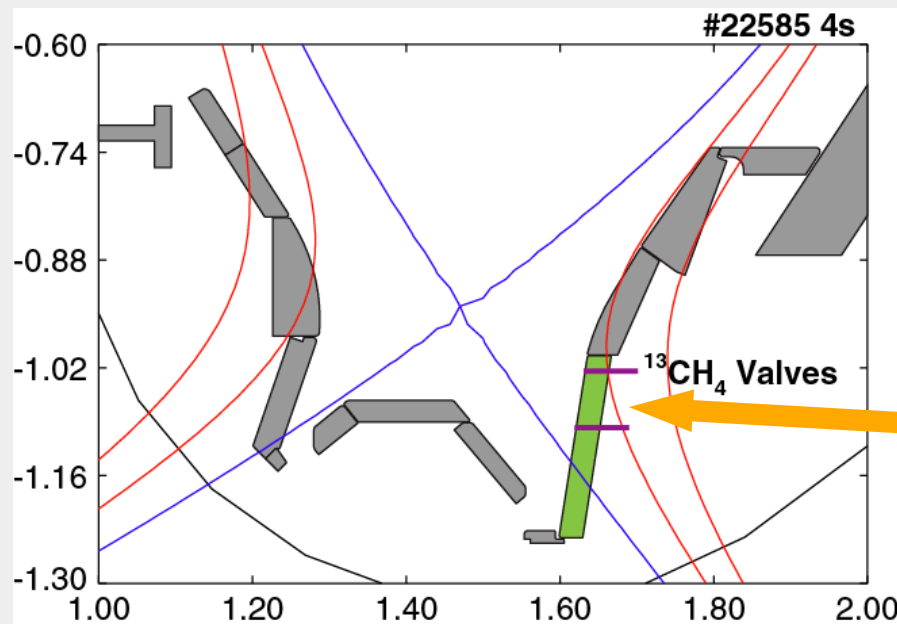
Example: ^{13}C injection in JET



J. Strachan

Benchmarking EDGE2D fluid code model

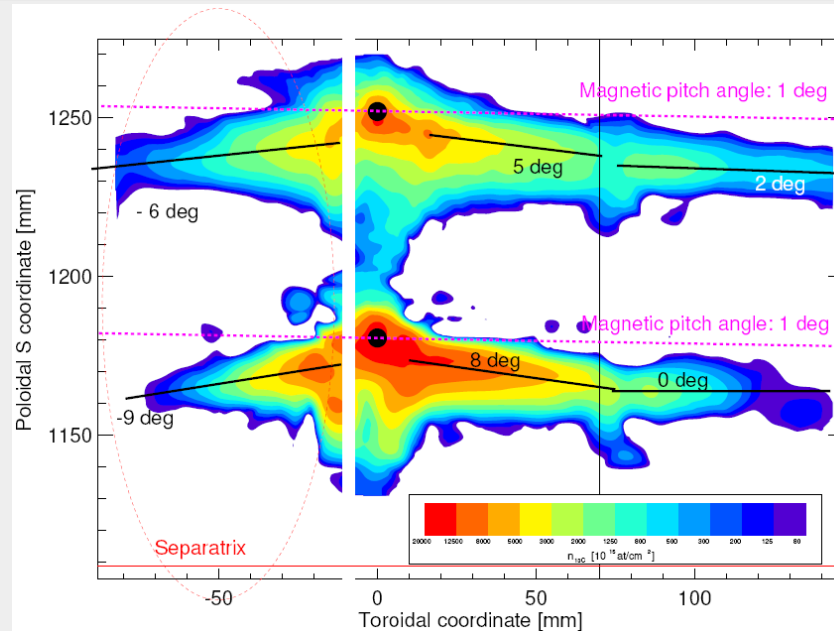
Example: $^{13}\text{CH}_4$ local injection in ASDEX Upgrade



- Puff trace amounts of $^{13}\text{CD}_4$ in series of similar discharges and measure local ^{13}C deposition 2D-distribution at retrieved tiles.
- ↪ Benchmark data for ERO and for spectroscopic CD flux

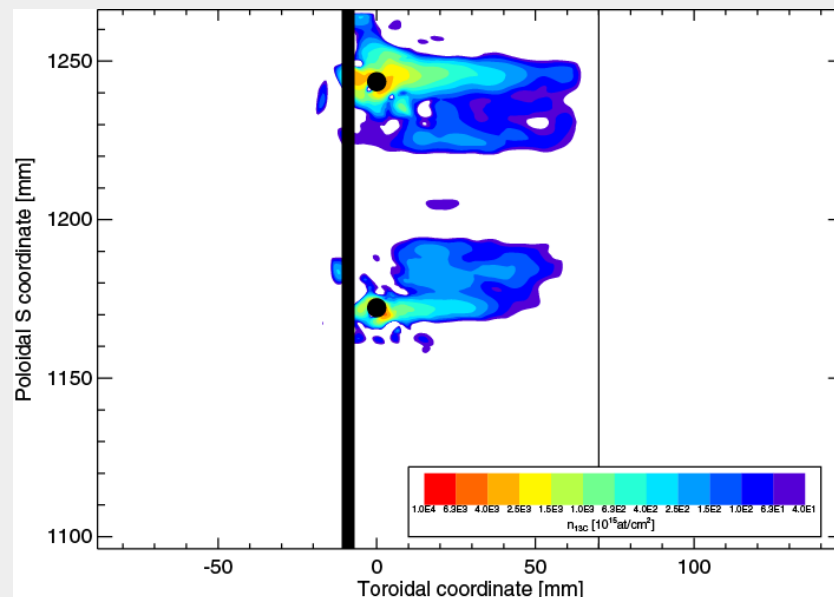
measurements

Example: $^{13}\text{CH}_4$ local injection in ASDEX Upgrade



- 11 L-mode discharges
- $^{13}\text{CH}_4$ puff 1.6–4.6 s

Reversal of deposition shift at B-field reversal
 ↗ Shift due to ExB drift



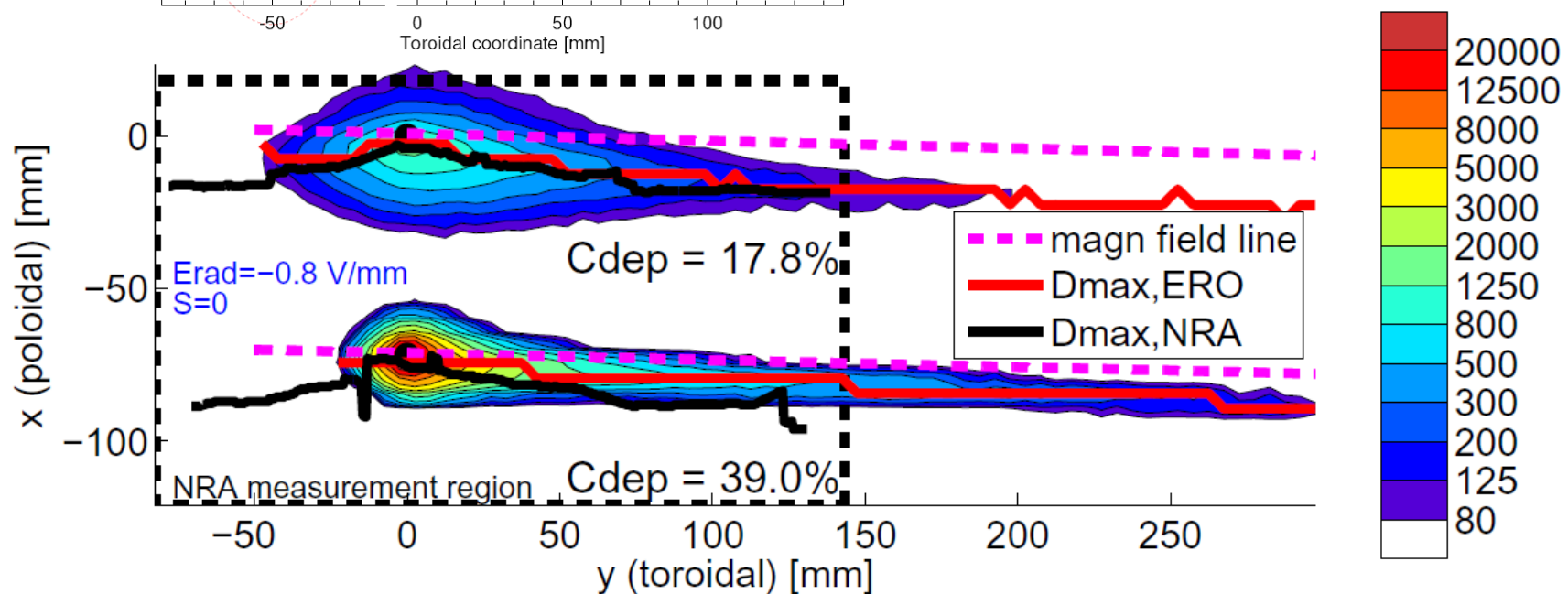
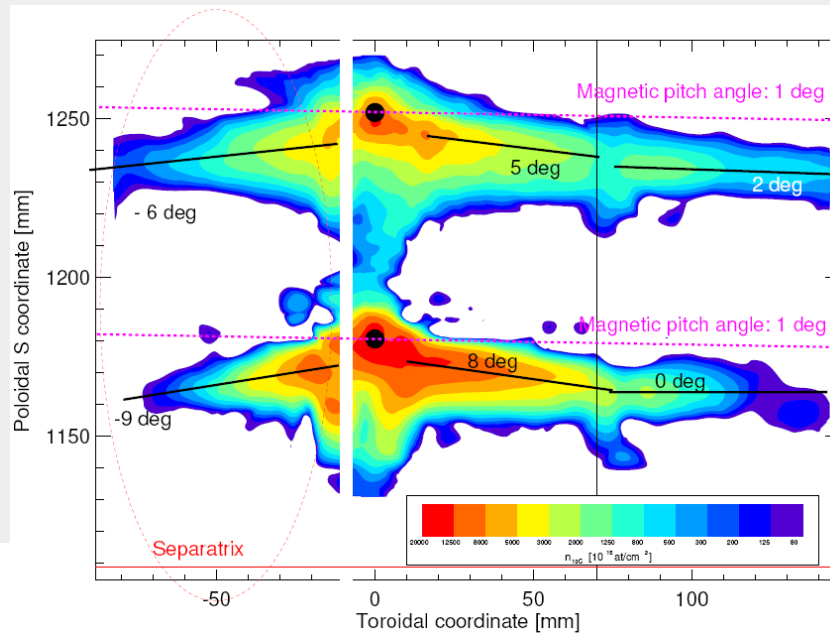
- 3 L-mode discharges
- $^{13}\text{CH}_4$ puff 1.6–4.3 s

Reversed B_t, I_p

Example: 13CH4 local injection in ASDEX Upgrade

L. Aho-Mantila

ERO recreates both $E \times B$ drift and upstream deposition due to neutral dissociation products



Advantages:

Well defined particular discharge scenario for code benchmarking

Very sensitive quantification of tracer materials

Disadvantages:

Provides only net-deposition data. Re-erosion only by indirect evidence

Only one scenario per campaign

Cover main chamber wall with Be by heavy Be evaporation.

Follow relaxation of Be/C wall sources, plasma concentration and QMB deposition towards steady state situation.

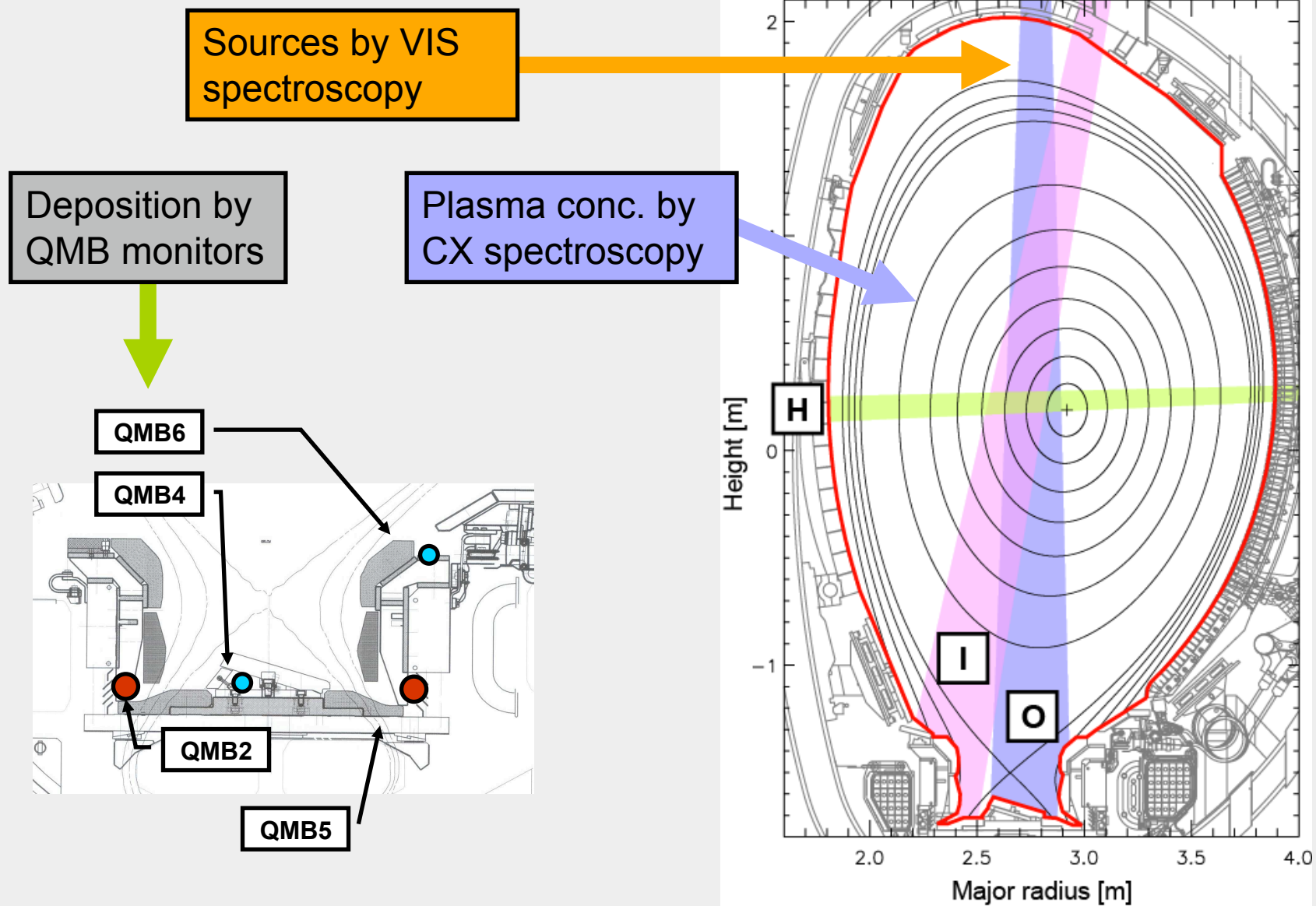
Compare to reference discharge immediately before Be evaporation.

Spectroscopic measurements allow to determine gross erosion flux.

Allows to study global screening by comparison with plasma impurity concentration.

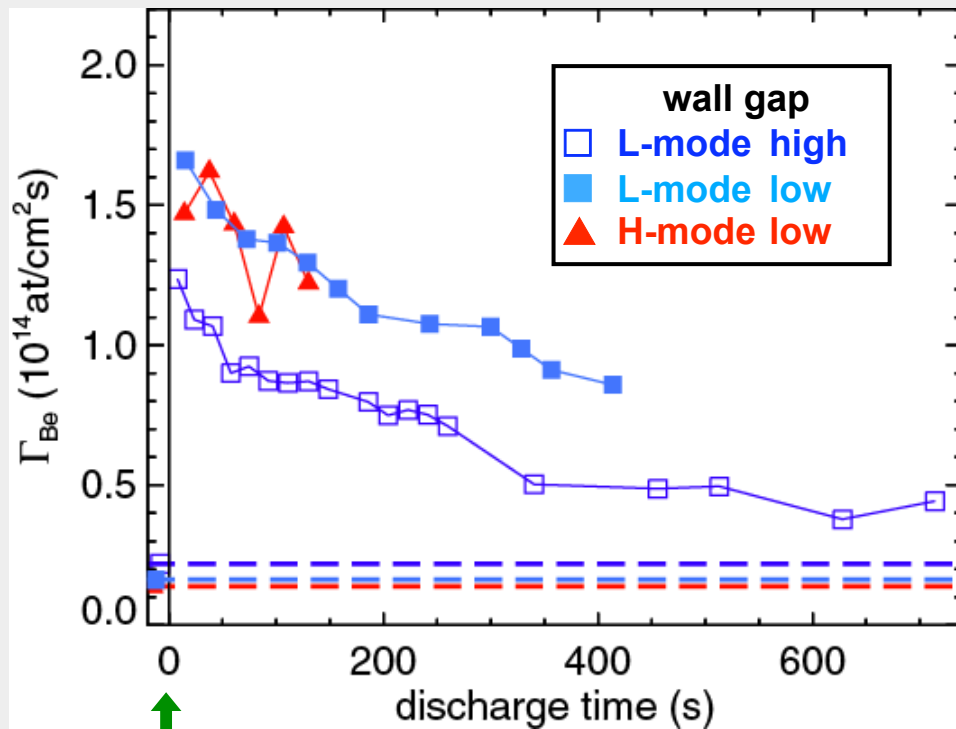
Evolution of wall composition provides information on material migration.

Diagnostic array

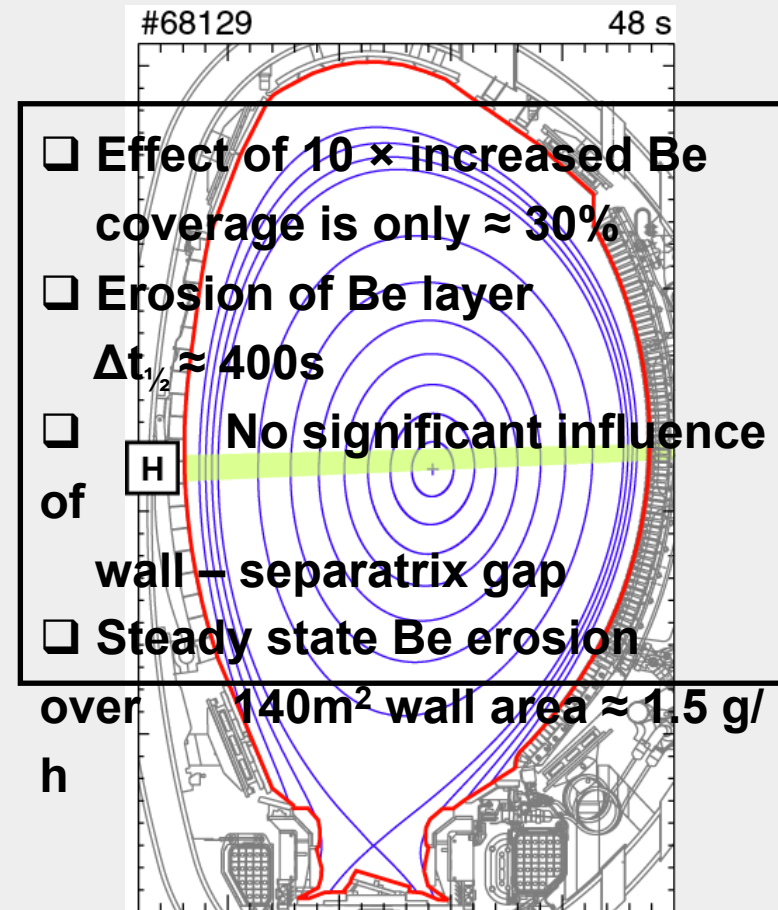


Evolution of Be wall sources

Local Be flux at first wall mid-plane from Be II line (527nm)

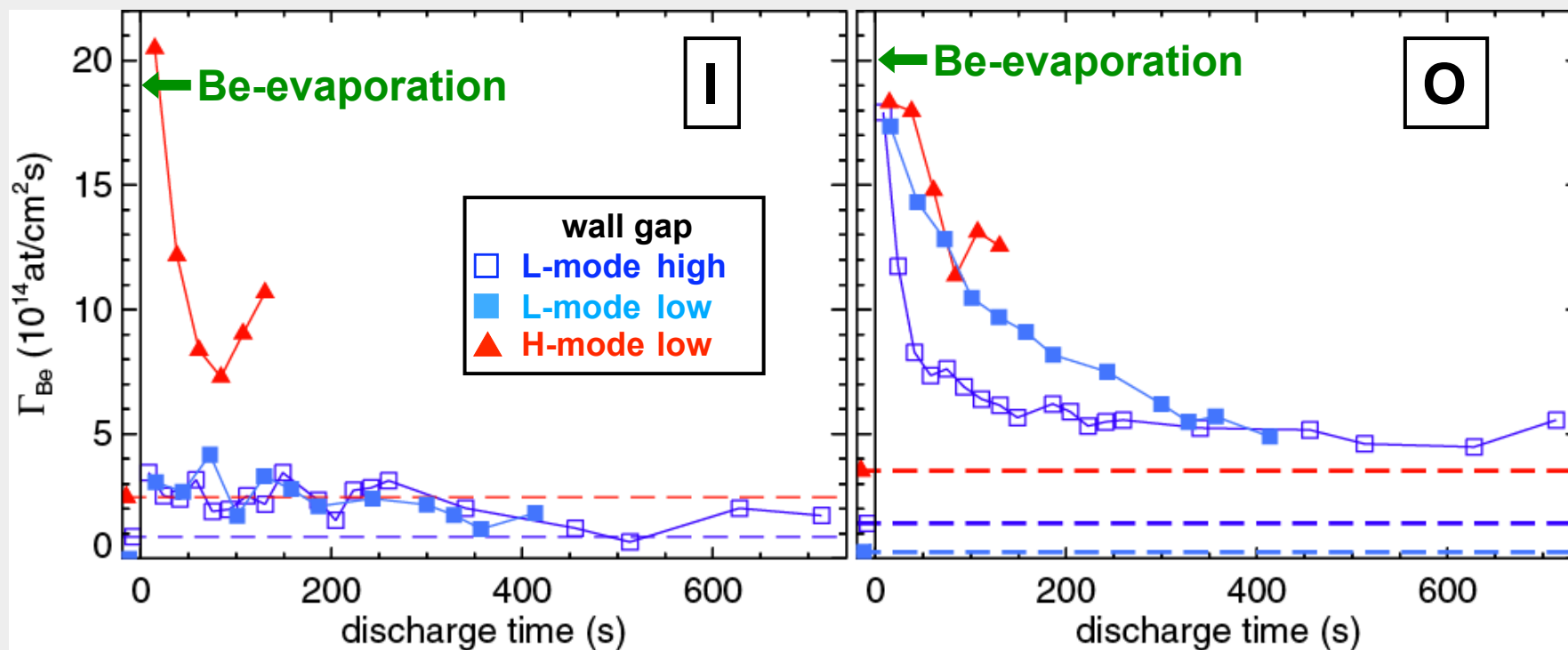


Be-evaporation



Evolution of Be divertor sources

Integrated Be flux from inner (I) and outer (O) divertor from Be II (527nm)

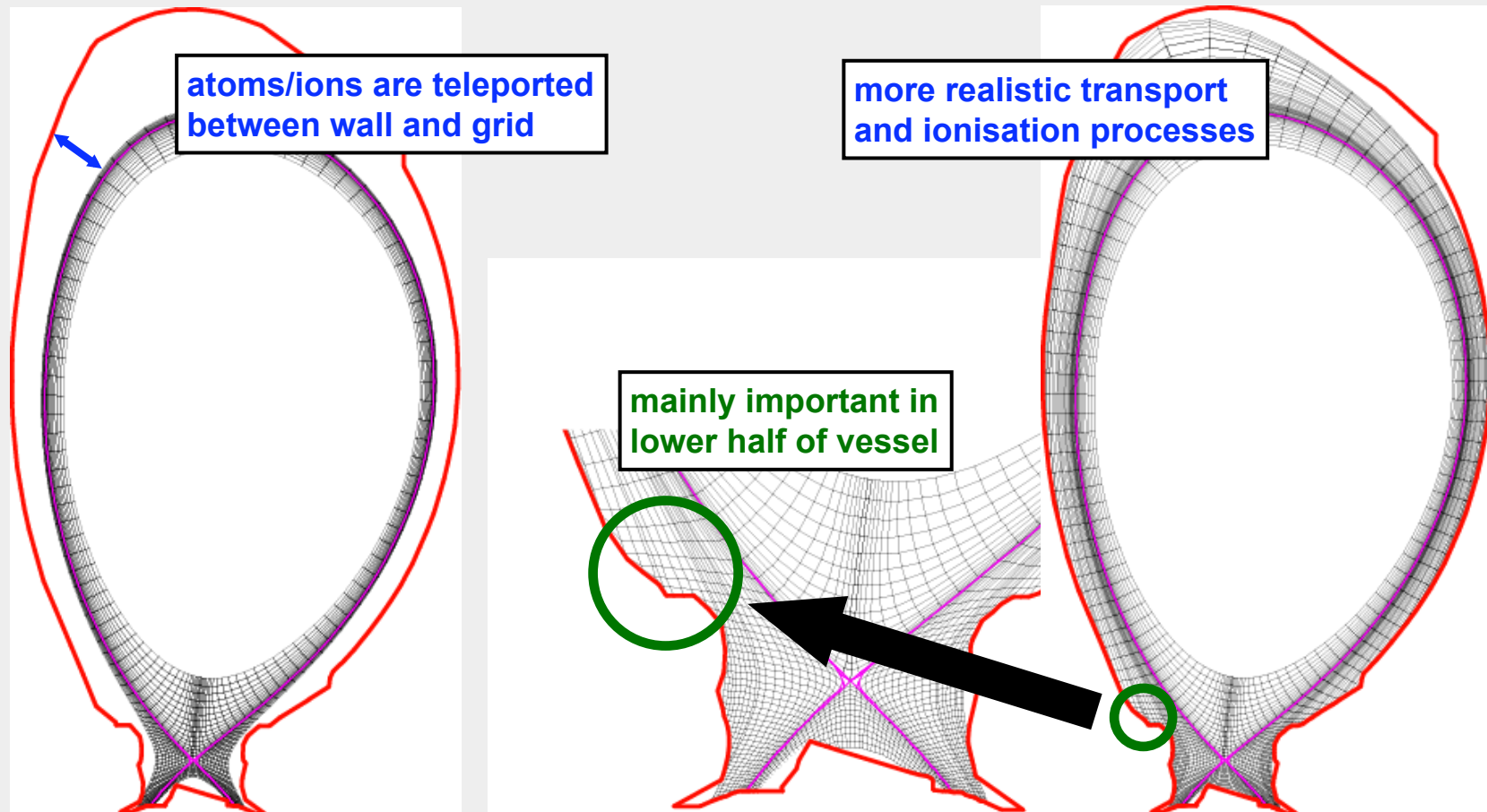


<ul style="list-style-type: none"> □ L-mode: Be flux ≈ constant ↘ Deposition zone □ H-mode: Strong decrease of Be flux ↘ Erosion zone 		<p>Wall gap: Be flux</p> <p>Mainly erosion of</p> <p>Be from wall</p> <p>Large gap: Be flux ≈ constant after 100s</p>
---	--	---

Modelling wall composition change by migration

- ❑ Standard grid topology is restricted to plasma-wall contact at target plates
- ⇒ Missing processes at "white spots":
 - \parallel and \perp transport to wall
 - ionisation & transport of eroded atoms

- ❑ Extend grid and tailor to 1st wall
- ❑ Fill with plasma using extrapolation from original grid



Advantages:

Well defined particular discharge scenario for code benchmarking
Trace several materials simultaneously

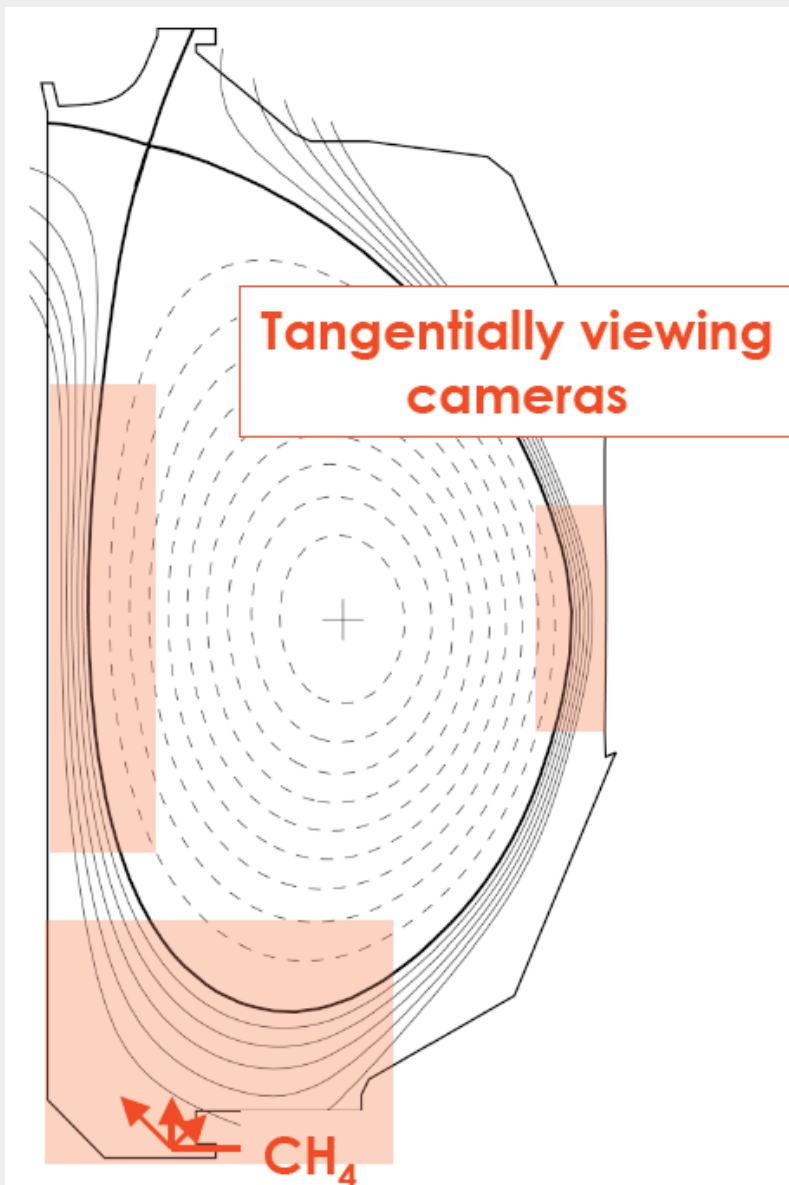
Disadvantages:

Provides only gross erosion data. Deposition only by indirect evidence
Quantitative impurity flux quantification requires local plasma parameters

Direct observation of impurity radiation during injection

Spectroscopic measurements allow to determine spatial distribution of emission by successive ionisation states

Allows to directly observe the influence of transport

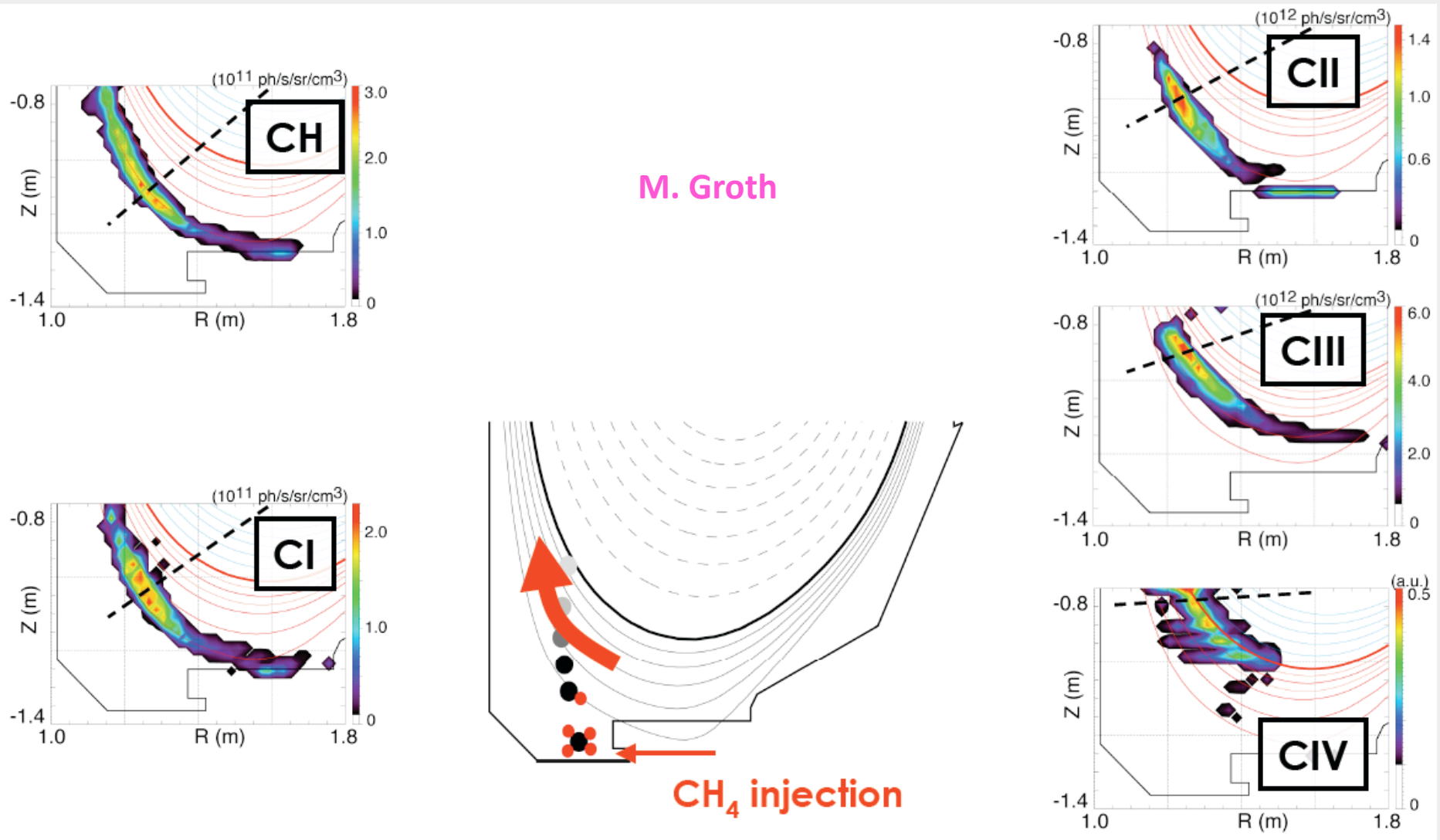


- **Principal flow measurements in the plasma crown**
 - Multi-tipped, reciprocating Langmuir probe: parallel-**B** v_{D^+}
 - Passive Doppler spectroscopy: parallel-**B** v_{C^+} , $v_{C^{2+}}$
- **Toroidally symmetric injection of CH_4 from lower outer pumping plenum + tangential cameras**
 - Emission profiles: direction of low charge-state carbon flow
 - Order-of-magnitude estimate of C^+ poloidal velocity

M. Groth

Example: carbon flow measurements in DIII-D

Carbon emission profiles of CH₄ break-up are progressively shifted radially inward and poloidally toward inner plate



Overview and rationale

Material transport processes

Particle collisions

Plasma turbulence

Experiments

Phenomenological observations

Specific experiments

Summary and outlook

Experiment side

Implement new PSI and impurity transport diagnostics to study time-dependent processes in single discharges

Improve diagnostics for characterisation of incident plasma flux

Modelling side

Get complete treatment of transport processes

Coupled codes for plasma and material side

Extend computational domain for plasma towards entire 1st wall

Develop 3D codes for near wall domain